fractal and fractional

Article

The Multi-Switching Sliding Mode Combination Synchronization of Fractional Order Non-Identical Chaotic System with Stochastic Disturbances and Unknown Parameters

Weiqiu Pan [1], Tianzeng Li [1,2,*] and Yu Wang [1]

[1] College of Mathematics and Statistics, Sichuan University of Science and Engineering, Zigong 643000, China; pwq237609@163.com or 31907010403@suse.edu.cn (W.P.); wangyu_813@163.com or stwangyu@suse.edu.cn (Y.W.)
[2] South Sichuan Center for Applied Mathematics, Yibin 644000, China
* Correspondence: litianzeng27@163.com or litianzeng@suse.edu.cn

Abstract: This paper deals with the issue of the multi-switching sliding mode combination synchronization (MSSMCS) of fractional order (FO) chaotic systems with different structures and unknown parameters under double stochastic disturbances (SD) utilizing the multi-switching synchronization method. The stochastic disturbances are considered as nonlinear uncertainties and external disturbances. Our theoretical part considers that the drive-response systems have the same or different dimensions. Firstly, a FO sliding surface is established in terms of the fractional calculus. Secondly, depending on the FO Lyapunov stability theory and the sliding mode control technique, the multi-switching adaptive controllers (MSAC) and some suitable multi-switching adaptive updating laws (MSAUL) are designed. They can ensure that the state variables of the drive systems are synchronized with the different state variables of the response systems. Simultaneously, the unknown parameters are assessed, and the upper bound values of stochastic disturbances are examined. Selecting the suitable scale matrices, the multi-switching projection synchronization, multi-switching complete synchronization, and multi-switching anti-synchronization will become special cases of MSSMCS. Finally, examples are displayed to certify the usefulness and validity of the scheme via MATLAB.

Keywords: fractional-order chaotic system; multi-switching combination synchronization (MSCS); adaptive sliding mode control; stochastic disturbance; unknown parameters

Citation: Pan, W.; Li, T.; Wang, Y. The Multi-Switching Sliding Mode Combination Synchronization of Fractional Order Non-Identical Chaotic System with Stochastic Disturbances and Unknown Parameters. *Fractal Fract.* **2022**, *6*, 102. https://doi.org/10.3390/fractalfract6020102

Academic Editors: Isabela Roxana Birs, Cristina I. Muresan and Clara Ionescu

Received: 7 January 2022
Accepted: 5 February 2022
Published: 11 February 2022

1. Introduction

Chaos is an inherent characteristic of nonlinear dynamic systems and a common phenomenon in real life. The chaotic phenomenon exhibited by the chaotic system is uncertain, unrepeatable, and unpredictable. Therefore, experts in mathematics and control have carried out a series of studies on the control and synchronization of chaotic systems. So far, some effective synchronization methods have been proposed, such as drive-response synchronization [1], projection synchronization [2,3], adaptive fuzzy synchronization [4–6], neural network synchronization [7,8], feedback synchronization [9], pulse synchronization [10,11], sliding mode synchronization [12,13], etc. People apply chaotic synchronization to secure communication, signal processing and life sciences, etc. Thus, chaos synchronization has gradually become a core research topic in the field of control science. Because chaotic systems are extremely sensitive to initial values, they are often subject to some SD. Whether it is the uncertainties within the system, such as parameter uncertainties, nonlinear uncertainties, or external disturbances, they cause an effect on the stability of the system.

In the beginning, these synchronization methods are used by people to research the synchronization of single-drive system and single-response system [14–19]. Gradually, some scholars have considered the influence of SD on this basis [20–27]. Since Runzi et al. [28]

revealed the combination synchronization scheme, the synchronization of multi-drive and multi-response systems, multi-drive and single-response systems, single-drive and multi-response systems are suggested. Later, some new synchronization schemes appeared and have been developed by leaps and bounds, such as the combination-combination synchronization [29–32], compound synchronization [33–35] and double compound synchronization [36,37], etc. It will be a major breakthrough in chaos synchronization. A major advantage of these new synchronization schemes is that they can ensure the information security. However, with the increasing complexity of signal transmission, how to strengthen information security is a thought-provoking problem.

In recent years, a new multi-switching combination synchronization (MSCS) scheme was analyzed by Vincent U et al. [30], which means the state variables of the drive systems are synchronized with the different state variables of the response systems, breaking the conventional synchronization rules. Compared with the traditional synchronization or some extension of it, the MSCS scheme is very promising because it can provide greater security for secure communication. The topic of dual combination-combination multi-switching synchronization in terms of eight chaotic systems was solved in [38]. The global exponential MSCS was introduced in terms of three different chaotic systems [39]. Reference [40] solved the problem of MSCS between three different integer-order chaotic systems. Adopting adaptive control technology, reference [41] investigated the multi-switching combination-combination synchronization of four integer-order chaotic systems which parameters are fully unknown. An further work of [41] has been developed by [42], which is indicated as an integer-order time-delay chaotic system. Shafiq M et al. [43] proposed a robust adaptive multi-switching technology to solve the issue of anti-synchronization for unknown hyperchaotic systems under SD. The authors of references [44,45] considered the multi-switching synchronization of the single-drive and single-response system which the parameters are unknown. Their innovations lie in the orders of the drive-response systems are different in [44] and the dimensions are different in [45]. On the contrary, Chen et al. [46] considered the synchronization of multiple chaotic systems with unknown parameters and disturbances. It's a pity that the case of multi-switching is not considered. Although reference [47] took multi-switching scheme into account in terms of multiple chaotic systems, it does not consider the influence of unknown parameters and SD.

As we all know, sliding mode control is a useful tool for the fractional (or integer) order systems due to its strong robustness for the SD. Therefore, some scholars prefer to use sliding mode control technology to research the uncertain chaotic systems, such as, in [48], Modiri et al. have considered the fractional order uncertain chaotic systems and designed a fractional-order adaptive terminal sliding mode controller to estimate the upper bounds of stochastic disturbances. Sun et al. [49] have researched the synchronization of fractional-order chaotic systems with non-identical orders, unknown parameters and disturbances via sliding mode control. The issue of synchronization of a class of chaotic systems with disturbances and unknown parameters are focused where the disturbances are supposed as bounds [50]. In addition, some scholars proposes the fractional-order sliding mode control based on the disturbance observer to study the fractional order chaotic systems with SD [51–55]. It is a good idea to study the multi-switch synchronization of fractional-order chaotic systems under stochastic disturbance based on the sliding mode control.

Hence, in order to address this limitation, we plan to solve the multi-switching sliding mode combination synchronization (MSSMCS) of fractional order (FO) chaotic systems with different (or same) dimensions under double stochastic disturbances (SD). Meanwhile, the parameters of two drive systems and one response system are fully unknown. The double SD are considered as nonlinear uncertainties and external disturbances. In the light of Lyapunov stability theory and sliding mode control technique, we introduce two multi-switching adaptive controllers (MSAC) and some multi-switching adaptive updating laws (MSAUL) to realize the multi-switching synchronization of D-R systems and assess the unknown parameters. Numerical simulations via MATLAB demonstrate the multi-switching controllers we conducted have good robustness and anti-interference performance. There are three innovations points in this article. (a) On the basis of reference [45], the fractional-order chaotic system is considered. The combination synchronization has been extended to two drive systems and one response system. (b) The multi-switching sliding mode combination synchronization (MSSMCS) of fractional order (FO) chaotic systems with different dimensions under double stochastic disturbances (SD) is investigated for the first time. (c) Several existing synchronization schemes (projection synchronization, complete synchronization and anti-synchronization) are obtained as special cases of MSSMCS.

The rest of the paper is described as follows. In Section 2, some definitions and lemmas are introduced. In Section 3, the problem statements are given. In Section 4, the MSAC and MSAUL are designed for D-R systems with the same dimension. In Section 5, the MSAC and MSAUL are designed for D-R systems with different dimensions. In Section 6, the numerical simulations conducted that our method is effective and dependable. In Section 7, there is a conclusion.

2. Preliminaries

The fractional calculus is an ancient and "fresh" concept. As early as the establishment of integer calculus, some scholars began to consider its meaning. Up till the present moment, there are some commonly used types of fractional derivatives, such as the Riemann–Liouville (R-L), Caputo and Grunwald-Letnikov (G-L) derivative, etc. Among these definitions, Caputo's derivative definition is the most generally utilized.

Definition 1 ([56])**.** *The mathematical expression of the fractional integral of the function $f(t)$ is following*

$$I_t^{\alpha} f(t) = \frac{1}{\Gamma(\alpha)} \int_a^t \frac{f(v)}{(t-v)^{1-\alpha}} dv, \tag{1}$$

where $\Gamma(\alpha)$ indicates the Gamma function.

Definition 2 ([56])**.** *The mathematical expression of Caputo derivative with order α is given as*

$${}_a^C D_t^{\alpha} f(t) = \frac{1}{\Gamma(p-\alpha)} \int_a^t (t-v)^{p-\alpha-1} f^{(p)}(v) dv, \tag{2}$$

where $p-1 < \alpha < p, p \in \mathbb{Z}^+$.

Lemma 1 ([18])**.** *When $\boldsymbol{x}(t) \in \mathbb{R}^n$ has continuous first derivative, then*

$${}_a D_t^{\alpha} (\frac{1}{2} \boldsymbol{x}^T(t) Q \boldsymbol{x}(t)) \leq \boldsymbol{x}^T Q_a D_t^{\alpha} \boldsymbol{x}(t), \tag{3}$$

where $\alpha \in (0,1)$ and $Q \in R^n \times R^n$ indicates a positive definite matrix.

Considering that most of the things around us are nonlinear, we write the fractional order nonlinear system to be:

$${}_0 D_t^{\boldsymbol{\alpha}} \boldsymbol{x}(t) = \boldsymbol{f}(t, \boldsymbol{x}(t)), \tag{4}$$

where $\alpha \in (0,1)$, $\boldsymbol{f} = (f_1, f_2, \cdots, f_n)^T$, $\boldsymbol{x}(t) \in \mathbb{R}^n$. Additionally, $f : [t_0, \infty] \times \Omega \to \mathbb{R}^n$ meets Lipschitz conditions; the initial value is $x(t_0) = x_0, t_0 \geq 0$. The equilibrium point $\boldsymbol{x}^*$ of (4) can be obtained from $\boldsymbol{f}(\boldsymbol{x}^*) = 0$.

Theorem 1 ([57])**.** *Suppose that $\mathbb{D} \in \mathbb{R}^n$ is a domain that contains the origin. If there exists a locally bounded Lyapunov function $V(t, \boldsymbol{x}(t)) : [t_0, \infty] \times \mathbb{D} \to \mathbb{R}$, which meets the local Lipschitz condition about $\boldsymbol{x}$ adapting to*

$$\eta_1(\|\boldsymbol{x}(t)\|^a) \leq V(t,\boldsymbol{x}(t)) \leq \eta_2(\|\boldsymbol{x}(t)\|^{ab}),$$
$$_0D_t^\alpha V(t,\boldsymbol{x}(t)) \leq -\eta_3(\|\boldsymbol{x}(t)\|^{ab}), \tag{5}$$

where $\alpha \in (0,1)$, $a > 0$, $b > 0$, $\eta_i(i = 1,2,3) > 0$, then the system (4) is called Mittag–Leffler stable.

3. Problem Description

The FO D-R systems with SD are demonstrated as

$$_0D_t^{\boldsymbol{\alpha}}\boldsymbol{x}(t) = \boldsymbol{F}(\boldsymbol{x}(t))\boldsymbol{\theta} + \boldsymbol{f}(\boldsymbol{x}(t)) + \Delta\boldsymbol{f}(\boldsymbol{x}(t)) + \boldsymbol{d}(\boldsymbol{x},t), \tag{6}$$

$$_0D_t^{\boldsymbol{\alpha}}\boldsymbol{y}(t) = \boldsymbol{G}(\boldsymbol{y}(t))\boldsymbol{\beta} + \boldsymbol{g}(\boldsymbol{y}(t)) + \Delta\boldsymbol{g}(\boldsymbol{y}(t)) + \boldsymbol{D}(\boldsymbol{y},t), \tag{7}$$

where the systems (6), (7) are regarded as the drive systems. $\boldsymbol{x}(t) = (x_1,x_2,\cdots,x_m)^T$ and $\boldsymbol{y}(t) = (y_1,y_2,\cdots,y_m)^T$ are the state variables. $\boldsymbol{\theta} = (\theta_1,\theta_2,\cdots,\theta_m)^T$ and $\boldsymbol{\beta} = (\beta_1,\beta_2,\cdots,\beta_m)^T$ are the parameter vectors; $\boldsymbol{F}_k(\boldsymbol{x}(t)),(k = 1,2,\cdots,n)$ is the k th row of $n \times m$ matrix $\boldsymbol{F}(\boldsymbol{x}(t))$ and $\boldsymbol{G}_j(\boldsymbol{y}(t)),(j = 1,2,\cdots,n)$ is the j th row of $n \times m$ matrix $\boldsymbol{G}(\boldsymbol{y}(t))$ whose elements are continuous nonlinear functions; $\boldsymbol{f}(\boldsymbol{x}(t)) = (f_1,f_2,\cdots,f_m)^T, \boldsymbol{g}(\boldsymbol{y}(t)) = (g_1,g_2,\cdots,g_m)^T$ are the nonlinear continuous functions; $\boldsymbol{d}(\boldsymbol{x}(t)) = (\mathrm{d}_1,\mathrm{d}_2,\cdots,\mathrm{d}_\mathrm{m})^T$, $\boldsymbol{D}(\boldsymbol{y}(t)) = (D_1,D_2,\cdots,D_m)^T$ are the external disturbances; $\Delta\boldsymbol{f}(\boldsymbol{x}(t)) = (\Delta f_1,\Delta f_2,\cdots,\Delta f_m)^T$, $\Delta\boldsymbol{g}(\boldsymbol{y}(t)) = (\Delta g_1,\Delta g_2,\cdots,\Delta g_m)^T$ are the nonlinear uncertainties; $\boldsymbol{\alpha} \in (0,1)$ represents the fractional order.

$$_0D_t^{\boldsymbol{\alpha}}\boldsymbol{z}(t) = \boldsymbol{H}(\boldsymbol{z}(t))\boldsymbol{\vartheta} + \boldsymbol{h}(\boldsymbol{z}(t)) + \Delta\boldsymbol{h}(\boldsymbol{z}(t)) + \boldsymbol{\mu}(\boldsymbol{z},t) + \boldsymbol{u}(t), \tag{8}$$

where the system (8) is regarded as the response system. $\boldsymbol{z}(t) = (z_1,z_2,\cdots,z_n)^T$ and $\boldsymbol{\vartheta} = (\vartheta_1,\vartheta_2,\cdots,\vartheta_n)^T$ are the state variable and parameter vector; $\boldsymbol{H}_i(\boldsymbol{z}(t)),(i = 1,2,\cdots,n)$ is the i th row of $n \times n$ matrix $\boldsymbol{H}(\boldsymbol{z}(t))$ whose elements are continuous nonlinear functions; $\boldsymbol{h}(\boldsymbol{z}(t)) = (h_1,h_2,\cdots,h_n)^T$ are the nonlinear continuous functions; $\boldsymbol{\mu}(\boldsymbol{z}(t)) = (\mu_1,\mu_2,\cdots,\mu_n)^T$ are the external disturbances; $\Delta\boldsymbol{h}(\boldsymbol{z}(t)) = (\Delta h_1,\Delta h_2,\cdots,\Delta h_n)^T$ are the nonlinear uncertainties. $\boldsymbol{u}(t) = (u_1,u_2,\cdots,u_n)^T$ represent the controller.

Remark 1. *It is worth noting that $\boldsymbol{x}(t),\boldsymbol{y}(t) \in \mathbb{R}^m$, $\boldsymbol{z}(t) \in \mathbb{R}^n$, $m = n$ or $m \neq n$; and the parameters of the D-R systems are unknown. We use $\hat{\boldsymbol{\theta}}$, $\hat{\boldsymbol{\beta}}$, $\hat{\boldsymbol{\vartheta}}$ to represent the estimation of parameters $\boldsymbol{\theta}$, $\boldsymbol{\beta}$, $\boldsymbol{\vartheta}$.*

Definition 3. *If there exist three constant matrices $A \in \mathbb{R}^{n\times m}, B \in \mathbb{R}^{n\times m}, C \in \mathbb{R}^{n\times n}, C \neq 0$ such that*

$$\lim_{t\to\infty}\|\boldsymbol{e}\| = \lim_{t\to\infty}\|C\boldsymbol{z} - (B\boldsymbol{y} + A\boldsymbol{x})\| = 0, \tag{9}$$

then the drive systems (6), (7) and response system (8) can be reach combination synchronization.

Remark 2. *If $A = (a_{vk})_{n\times m}, B = (b_{wj})_{n\times m}, C = (c_{li})_{n\times n}, C \neq 0$, we can redefined the error system (9) as*

$$\lim_{t\to\infty} {}^{(lwv)}e_p = \lim_{t\to\infty}[\sum_{i=1}^{n}(c_{li}z_i) \; - \{\sum_{j=1}^{m}(b_{wj}y_j) + \sum_{k=1}^{m}(a_{vk}x_k)\}], \tag{10}$$

where $p,i,j,k,l,w,v \in (1,2,\cdots,n)$. The subscript (p) represents p th error component of $\boldsymbol{e}$; the (ijk) represents i th components of $\boldsymbol{z}$, j th components of $\boldsymbol{y}$, and k th components of $\boldsymbol{x}$, respectively; the superscript (lwv) represents l th row of matrix C, w th row of matrix B, and v th row of matrix

A, respectively (l, w, v means the switching mode). Suppose that $l = w = v$, then the error variables are expressed in the form of Definition 3; if $l \neq w \neq v$, Definition 3 will no longer apply.

Definition 4. *We redefine the error state in Definition 3 as*

$$\lim_{t\to\infty} {}^{(lwv)}e_p = \lim_{t\to\infty}[\sum_{i=1}^{n}(c_{li}z_i) \; - \{\sum_{j=1}^{m}(b_{wj}y_j) + \sum_{k=1}^{m}(a_{vk}x_k)\}] = 0, \tag{11}$$

then the drive systems (6), (7) and the response system (8) realize the MSCS, where $l = w \neq v$ or $l \neq w = v$ or $l = v \neq w$ or $l \neq w \neq v$.

Remark 3. *The matrices $A \in \mathbb{R}^{n\times m}, B \in \mathbb{R}^{n\times m}, C \in \mathbb{R}^{n\times n}$, $C \neq 0$ are hailed as the scaling matrices. Furthermore, they can be either constant matrices or the functions with regard to state variables $\boldsymbol{x}$, $\boldsymbol{y}$, $\boldsymbol{z}$.*

Remark 4. *If $A = B = C = I$, the MSCS becomes the multi-switching combination complete synchronization; if $A = 0, B = C = I$ or $B = 0, A = C = I$, the MSCS becomes the multi-switching complete synchronization.*

Remark 5. *If $A = B = -I, C = I$, the MSCS becomes the multi-switching combination anti-synchronization; if $A = 0, B = -I, C = I$ or $B = 0, A = -I, C = I$, the MSCS becomes the multi-switching anti-synchronization.*

Remark 6. *If $A \neq I, B \neq I, C = I$, the MSCS becomes the multi-switching combination projective synchronization; if $A = 0, B \neq I, C = I$ or $B = 0, A \neq I, C = I$, the MSCS becomes the multi-switching projective synchronization.*

Remark 7. *If $A = B = 0$, the MSCS becomes a chaos control problem.*

4. The Synchronization of Multi-Switching FO Chaotic System with Same Dimension

In Section 4, the MSSMCS of FO chaotic systems with same dimension is formulated. It means that the dimension of D-R systems (6)–(8) satisfies $m = n$. Thus, the scaling matrices A, B, C are given as diagonal matrices. Firstly, we know that even if a chaotic system is slightly disturbed, its state orbits will change drastically over time. Therefore, it is crucial to suppose them as bounded. Then, we designed appropriate multi-switching adaptive controllers (MSAC) and some multi-switching adaptive updating laws (MSAUL) to realize the synchronization of the D-R systems, which are proved in Theorem 2.

When we choose $m = n$ and the diagonal matrices $A = diag(a_{11}, a_{22}, \cdots, a_{nn})$, $B = diag(b_{11}, b_{22}, \cdots, b_{nn})$, $C = diag(c_{11}, c_{22}, \cdots, c_{nn})$, the error system (11) can be described as

$$\lim_{t\to\infty} {}^{(ijk)}e_p = \lim_{t\to\infty}[c_{ii}z_i - (b_{jj}y_j + a_{kk}x_k)] = 0, \tag{12}$$

where $i, j, k, p \in (1, 2, \cdots, n)$, $i = j \neq k$ or $i \neq j = k$ or $i = j \neq k$ or $i \neq j \neq k$. The subscript (p) represents p th error component of $\boldsymbol{e}$; the superscript (ijk) represents i th components of $\boldsymbol{z}$, j th components of $\boldsymbol{y}$, and k th components of $\boldsymbol{x}$.

Assumption 1. *Assume the external disturbances $\mathrm{d_k}$, D_j, μ_i, uncertain nonlinear vectors Δf_k, Δg_j, Δh_i all have a bounded norm. Namely, there are suitable positive constants ${}^{(ijk)}r_p$, ${}^{(ijk)}q_p$ that satisfy*

$$\begin{aligned} |c_{ii}\mu_i - (b_{jj}D_j + a_{kk}\mathrm{d_k})| &\leq {}^{(ijk)}r_p, \\ |c_{ii}\Delta h_i - (b_{jj}\Delta g_j + a_{kk}\Delta f_k)| &\leq {}^{(ijk)}q_p. \end{aligned} \tag{13}$$

where $p = 1, 2, \cdots, n$, $i = j \neq k$ or $i \neq j = k$ or $i = j \neq k$ or $i \neq j \neq k$.

Remark 8. *The positive constants* ${}^{(ijk)}r_p$, ${}^{(ijk)}q_p$ *are unknown.* ${}^{(ijk)}\hat{r}_p$, ${}^{(ijk)}\hat{q}_p$ *are used to represent the estimation of parameters* ${}^{(ijk)}r_p$, ${}^{(ijk)}q_p$.

According to the definition of the error vector (12), we get the FO error system as

$$\begin{aligned} {}_0D_t^{\alpha}\{{}^{(ijk)}e_p\} &= c_{ii}\{{}_0D_t^{\alpha}z_i\} - b_{jj}\{{}_0D_t^{\alpha}y_j\} - a_{kk}\{{}_0D_t^{\alpha}x_k\} \\ &= c_{ii}\boldsymbol{H}_i(z(t))\boldsymbol{\vartheta} + c_{ii}h_i(z(t)) + c_{ii}\Delta h_i(z(t)) + c_{ii}\mu_i(z,t) + c_{ii}\{{}^{(ijk)}u_p\} \\ &\quad - b_{jj}\boldsymbol{G}_j(y(t))\boldsymbol{\beta} - b_{jj}g_j(y(t)) - b_{jj}\Delta g_j(y(t)) - b_{jj}D_j(y,t) \\ &\quad - a_{kk}\boldsymbol{F}_k(x(t))\boldsymbol{\theta} - a_{kk}f_k(x(t)) - a_{kk}\Delta f_k(x(t)) - a_{kk}\mathrm{d}_\mathrm{k}(x,t). \end{aligned} \tag{14}$$

For convenience, we define the errors of unknown parameters $\boldsymbol{\theta}, \boldsymbol{\beta}, \boldsymbol{\vartheta}$, ${}^{(ijk)}r_p$, ${}^{(ijk)}q_p$ as $\tilde{\boldsymbol{\theta}} = \hat{\boldsymbol{\theta}} - \boldsymbol{\theta}$, $\tilde{\boldsymbol{\beta}} = \hat{\boldsymbol{\beta}} - \boldsymbol{\beta}$, $\tilde{\boldsymbol{\vartheta}} = \hat{\boldsymbol{\vartheta}} - \boldsymbol{\vartheta}$, ${}^{(ijk)}\tilde{r}_p = {}^{(ijk)}\hat{r}_p - {}^{(ijk)}r_p$, ${}^{(ijk)}\tilde{q}_p = {}^{(ijk)}\hat{q}_p - {}^{(ijk)}q_p$. When the sliding mode surface is designed as ${}^{(ijk)}s_p = \lambda\{{}^{(ijk)}e_p\}$, we can get the following MSAC (15) and MSAUL (18):

$$\begin{aligned} {}^{(ijk)}u_p = \frac{1}{c_{ii}}\{&-c_{ii}h_i + b_{jj}g_j + a_{kk}f_k + a_{kk}\boldsymbol{F}_k(x(t))\hat{\boldsymbol{\theta}} + b_{jj}\boldsymbol{G}_j(y(t))\hat{\boldsymbol{\beta}} \\ &- c_{ii}\boldsymbol{H}_i(z(t))\hat{\boldsymbol{\vartheta}} - ({}^{(ijk)}r_p + {}^{(ijk)}q_p)sgn({}^{(ijk)}s_p) - k_1 sgn({}^{(ijk)}s_p)\}, \end{aligned} \tag{15}$$

where λ, k_1 are constants. Substituting (15) into Equation (14), we obtain

$$\begin{aligned} {}_0D_t^{\alpha}\{{}^{(ijk)}e_p\} =& -c_{ii}\boldsymbol{H}_i(z(t))\tilde{\boldsymbol{\vartheta}} + b_{jj}\boldsymbol{G}_j(y(t))\tilde{\boldsymbol{\beta}} + a_{kk}\boldsymbol{F}_k(x(t))\tilde{\boldsymbol{\theta}} \\ &+ \{c_{ii}\Delta h_i(z(t)) - b_{jj}\Delta g_j(y(t)) - a_{kk}\Delta f_k(x(t))\} + \{c_{ii}\mu_i(z,t) \\ &- b_{jj}D_j(y,t) - a_{kk}\mathrm{d}_\mathrm{k}(x,t)\} - ({}^{(ijk)}r_p + {}^{(ijk)}q_p)sgn({}^{(ijk)}s_p) \\ &- k_1 sgn({}^{(ijk)}s_p). \end{aligned} \tag{16}$$

Therefore, a column vector representing the general form of the error system (16), whose elements are chosen arbitrarily form ${}^{(ijk)}e$ (i.e., when $i = 2, j = 3, k = 1$, an error mode is generated ${}^{(231)}e$) can be obtained the following form:

$$\begin{aligned} {}_0D_t^{\boldsymbol{\alpha}}\boldsymbol{e}(t) =& -C\boldsymbol{H}(z(t))\tilde{\boldsymbol{\vartheta}} + B\boldsymbol{G}(y(t))\tilde{\boldsymbol{\beta}} + A\boldsymbol{F}(x(t))\tilde{\boldsymbol{\theta}} + C\Delta\boldsymbol{h}(z(t)) - B\Delta\boldsymbol{g}(y(t)) \\ &- A\Delta\boldsymbol{f}(x(t)) + C\boldsymbol{\mu}(z,t) - B\boldsymbol{D}(y,t) - A\boldsymbol{d}(x,t) - (\boldsymbol{r}+\boldsymbol{q}) \circ sgn(\boldsymbol{s}) - k_1 sgn(\boldsymbol{s}). \end{aligned} \tag{17}$$

where $\circ$ represents the Hadamard product operator, $\boldsymbol{r} = ({}^{(ijk)}r_1, {}^{(ijk)}r_2, \cdots, {}^{(ijk)}r_p)$, $\boldsymbol{q} = ({}^{(ijk)}q_1, {}^{(ijk)}q_2, \cdots, {}^{(ijk)}q_p)$, $A = diag(a_{11}, a_{22}, \cdots, a_{nn})$, $B = diag(b_{11}, b_{22}, \cdots, b_{nn})$, $C = diag(c_{11}, c_{22}, \cdots, c_{nn})$.

The MSAUL with regard to unknown parameters $\boldsymbol{\theta}, \boldsymbol{\beta}, \boldsymbol{\vartheta}$, ${}^{(ijk)}r_p$, ${}^{(ijk)}q_p$ are selected as

$$\begin{aligned} &{}_0D_t^{\alpha}\hat{\boldsymbol{\theta}} = -\lambda\boldsymbol{F}^T(x(t))A^T\boldsymbol{s} - \varphi_1 sgn(\tilde{\boldsymbol{\theta}})|(\tilde{\boldsymbol{\theta}})|^w, \\ &{}_0D_t^{\alpha}\hat{\boldsymbol{\beta}} = -\lambda\boldsymbol{G}^T(y(t))B^T\boldsymbol{s} - \varphi_2 sgn(\tilde{\boldsymbol{\beta}})|(\tilde{\boldsymbol{\beta}})|^w, \\ &{}_0D_t^{\alpha}\hat{\boldsymbol{\vartheta}} = \lambda\boldsymbol{H}^T(z(t))C^T\boldsymbol{s} - \varphi_3 sgn(\tilde{\boldsymbol{\vartheta}})|(\tilde{\boldsymbol{\vartheta}})|^w, \\ &{}_0D_t^{\alpha}\{{}^{(ijk)}\hat{r}_p\} = m_1\lambda|{}^{(ijk)}s_p|, \\ &{}_0D_t^{\alpha}\{{}^{(ijk)}\hat{q}_p\} = m_2\lambda|{}^{(ijk)}s_p|, \end{aligned} \tag{18}$$

where $m_1, m_2, \varphi_1, \varphi_2, \varphi_3, w$ are positive constants and a column vector representing the general form of sliding mode surface ${}^{(ijk)}s_p = \lambda\{{}^{(ijk)}e_p\}$ can be obtained as $\boldsymbol{s} = \lambda\boldsymbol{e}$, $p = 1, 2, \cdots, n$.

Theorem 2. *For any given initial conditions $\boldsymbol{x}(0), \boldsymbol{y}(0), \boldsymbol{z}(0)$, if the Assumption 1 (13) is hold, the synchronization error system (12) will achieve the multi-switching sliding mode combination synchronization (MSSMCS) via the multi-switching adaptive controller (MSAC) (15) and multi-switching adaptive updating laws (MSAUL) (18).*

Proof. Adopting the Lyapunov function as:

$$V = \frac{1}{2}\boldsymbol{s}^T\boldsymbol{s} + \frac{1}{2}\tilde{\boldsymbol{\theta}}^T\boldsymbol{\theta} + \frac{1}{2}\tilde{\boldsymbol{\beta}}^T\boldsymbol{\beta} + \frac{1}{2}\tilde{\boldsymbol{\vartheta}}^T\boldsymbol{\vartheta} + \frac{1}{2m_1}\sum_{p=1}^{n}\{^{(ijk)}\tilde{r}_p^2\} + \frac{1}{2m_2}\sum_{p=1}^{n}\{^{(ijk)}\tilde{q}_p^2\}. \tag{19}$$

Taking the α derivative

$$\begin{aligned} {}_0D_t^\alpha V(t, \boldsymbol{x}(t)) \leq &\boldsymbol{s}^T{}_0D_t^\alpha\boldsymbol{s} + \tilde{\boldsymbol{\theta}}^T{}_0D_t^\alpha\hat{\boldsymbol{\theta}} + \tilde{\boldsymbol{\beta}}^T{}_0D_t^\alpha\hat{\boldsymbol{\beta}} + \tilde{\boldsymbol{\vartheta}}^T{}_0D_t^\alpha\hat{\boldsymbol{\vartheta}} \\ &+ \frac{1}{m_1}\sum_{p=1}^{n}\{^{(ijk)}\tilde{r}_p\}{}_0D_t^\alpha\{^{(ijk)}\hat{r}_p\} + \frac{1}{m_2}\sum_{p=1}^{n}\{^{(ijk)}\tilde{q}_p\}{}_0D_t^\alpha\{^{(ijk)}\hat{q}_p\}. \end{aligned} \tag{20}$$

Then substituting the Equation (17) and the MSAUL (18) into Equation (20), we obtain

$$\begin{aligned} {}_0D_t^\alpha V(t, \boldsymbol{x}(t)) \leq\ &\boldsymbol{s}^T\lambda\{-C\boldsymbol{H}(z(t))\tilde{\boldsymbol{\vartheta}} + B\boldsymbol{G}(y(t))\tilde{\boldsymbol{\beta}} + A\boldsymbol{F}(x(t))\tilde{\boldsymbol{\theta}} + C\Delta\boldsymbol{h}(z(t)) \\ &- B\Delta\boldsymbol{g}(y(t)) - A\Delta\boldsymbol{f}(x(t)) + C\boldsymbol{\mu}(z,t) - B\boldsymbol{D}(y,t) - A\boldsymbol{d}(x,t) \\ &- (\hat{\boldsymbol{r}} + \hat{\boldsymbol{q}}) \circ sgn(\boldsymbol{s}) - k_1 sgn(\boldsymbol{s})\} \\ &+ \tilde{\boldsymbol{\theta}}^T(-\lambda\boldsymbol{F}^T(x(t))A^T\boldsymbol{s} - \varphi_1 sgn(\tilde{\boldsymbol{\theta}})|(\tilde{\boldsymbol{\theta}})|^w) \\ &+ \tilde{\boldsymbol{\beta}}^T(-\lambda\boldsymbol{G}^T(y(t))B^T\boldsymbol{s} - \varphi_2 sgn(\tilde{\boldsymbol{\beta}})|(\tilde{\boldsymbol{\beta}})|^w) \\ &+ \tilde{\boldsymbol{\vartheta}}^T(\lambda\boldsymbol{H}^T(z(t))C^T\boldsymbol{s} - \varphi_3 sgn(\tilde{\boldsymbol{\vartheta}})|(\tilde{\boldsymbol{\vartheta}})|^w) \\ &+ \lambda\sum_{p=1}^{n}\{^{(ijk)}\tilde{r}_p\}|^{(ijk)}s_p| + \lambda\sum_{p=1}^{n}\{^{(ijk)}\tilde{q}_p\}|^{(ijk)}s_p| \\ \leq\ &\lambda\|\boldsymbol{s}\|\{\|C\Delta\boldsymbol{h}(z(t)) - B\Delta\boldsymbol{g}(y(t)) - A\Delta\boldsymbol{f}(x(t))\| \\ &+ \|C\boldsymbol{\mu}(z,t) - B\boldsymbol{D}(y,t) - A\boldsymbol{d}(x,t)\|\} \\ &- \lambda\boldsymbol{s}^T\{\hat{\boldsymbol{r}} + \hat{\boldsymbol{q}}\} \circ sgn(\boldsymbol{s}) - \lambda k_1\boldsymbol{s}^T sgn(\boldsymbol{s}) - \tilde{\boldsymbol{\theta}}^T(\varphi_1 sgn(\tilde{\boldsymbol{\theta}})|(\tilde{\boldsymbol{\theta}})|^w) \\ &- \tilde{\boldsymbol{\beta}}^T(\varphi_2 sgn(\tilde{\boldsymbol{\beta}})|(\tilde{\boldsymbol{\beta}})|^w) - \tilde{\boldsymbol{\vartheta}}^T(\varphi_3 sgn(\tilde{\boldsymbol{\vartheta}})|(\tilde{\boldsymbol{\vartheta}})|^w) \\ &+ \lambda\sum_{p=1}^{n}\{^{(ijk)}\tilde{r}_p\}|^{(ijk)}s_p| + \lambda\sum_{p=1}^{n}\{^{(ijk)}\tilde{q}_p\}|^{(ijk)}s_p|. \end{aligned} \tag{21}$$

Using the fact $\boldsymbol{s}^T sgn(\boldsymbol{s}) = \|\boldsymbol{s}\|$, $\tilde{\boldsymbol{\theta}}^T sgn(\tilde{\boldsymbol{\theta}}) = \|\tilde{\boldsymbol{\theta}}\|$, $\tilde{\boldsymbol{\beta}}^T sgn(\tilde{\boldsymbol{\beta}}) = \|\tilde{\boldsymbol{\beta}}\|$, $\tilde{\boldsymbol{\vartheta}}^T sgn(\tilde{\boldsymbol{\vartheta}}) = \|\tilde{\boldsymbol{\vartheta}}\|$, $\lambda\sum_{p=1}^{n}\{^{(ijk)}\tilde{r}_p\}|^{(ijk)}s_p| = \lambda\|r\|\|s\|$, $\lambda\sum_{p=1}^{n}\{^{(ijk)}\tilde{q}_p\}|^{(ijk)}s_p| = \lambda\|q\|\|s\|$ and the Assumption 1 (13) to (21) yields:

$$\begin{aligned} {}_0D_t^\alpha V(t, \boldsymbol{x}(t)) \leq\ &\lambda\|\boldsymbol{s}\|(\|\boldsymbol{r}\| + \|\boldsymbol{q}\|) - \lambda(\|\hat{\boldsymbol{r}}\| + \|\hat{\boldsymbol{q}}\|)\|\boldsymbol{s}\| - k_1\lambda\|\boldsymbol{s}\| \\ &+ \lambda|\boldsymbol{s}|(\|\tilde{\boldsymbol{r}}\| + \|\tilde{\boldsymbol{q}}\|) - \varphi_1|(\tilde{\boldsymbol{\theta}})|^{w+1} - \varphi_2|(\tilde{\boldsymbol{\beta}})|^{w+1} - \varphi_3|(\tilde{\boldsymbol{\vartheta}})|^{w+1} \\ \leq\ &-k_1\lambda\|\boldsymbol{s}\|, \end{aligned} \tag{22}$$

where $\|\bullet\|$ represents 1-norm, i.e., $\|\boldsymbol{x}\| = \sum_{i=1}^{n}|x_i|$ for $\boldsymbol{x} = (x_1, x_2, \cdots, x_n)$.

It is obvious that $V(t)$ is positive-definite and ${}_0D_t^\alpha V(t, \boldsymbol{x}(t))$ is negative semi-definite. Based on Barbalat's lemma [58], $\lim_{t\to\infty}{}_0D_t^\alpha V(t, \boldsymbol{x}(t)) = 0$ is obtained. We have $\lim_{t\to\infty}\|\boldsymbol{s}\| = 0$. Then, the trajectory of the error system is driven onto the predefined sliding surface, i.e., we can say that the MSSMCS of the drive systems (6), (7) and response system (8) is accomplished in terms of $m = n$. □

5. The Synchronization of Multi-Switching FO System with Different Dimensions

In Section 5, the MSSMCS of FO chaotic systems with different dimensions is formulated. It means that the dimensions of D-R systems (6)–(8) satisfy $m \neq n$. Thus, the scaling matrices A, B, C are given as non-diagonal matrices. We designed appropriate multi-switching adaptive controllers (MSAC) and some multi-switching adaptive updating laws (MSAUL) to realize the synchronization of the D-R systems which are proved in Theorem 3.

When we choose $m \neq n$ and the non-diagonal matrices $A = (a_{vk})_{n\times m}, B = (b_{wj})_{n\times m}$, $C = (c_{li})_{n\times n}, C \neq 0$, the form of the error system can be explained as (11), namely:

$$\lim_{t\to\infty} {}^{(lwv)}e_p = \lim_{t\to\infty}[\sum_{i=1}^{n}(c_{li}z_i) \; - \{\sum_{j=1}^{m}(b_{wj}y_j) + \sum_{k=1}^{m}(a_{vk}x_k)\}] = 0,$$

where the meaning of p, i, j, k, l, w, v can be seen (10), $l = w \neq v$ or $l \neq w = v$ or $l = v \neq w$ or $l \neq w \neq v$.

Assumption 2. *Assume the external disturbances d_k, D_j, μ_i, uncertain nonlinear vectors Δf_k, Δg_j, Δh_i all have a bounded norm. Namely, there are suitable positive constants ${}^{(lwv)}\rho_p$, ${}^{(lwv)}\varrho_p$ that satisfy*

$$\begin{aligned} \left|\sum_{i=1}^{n} c_{li}\mu_i - (\sum_{j=1}^{m} b_{wj}D_j + \sum_{k=1}^{m} a_{vk}\mathrm{d_k})\right| \leq {}^{(lwv)}\rho_p, \\ \left|\sum_{i=1}^{n} c_{li}\Delta h_i - (\sum_{j=1}^{m} b_{wj}\Delta g_j + \sum_{k=1}^{m} a_{vk}\Delta f_k)\right| \leq {}^{(lwv)}\varrho_p, \end{aligned} \tag{23}$$

where $p = 1, 2, \cdots, n$.

Remark 9. *The positive constants ${}^{(lwv)}\rho_p$, ${}^{(lwv)}\varrho_p$ are unknown, ${}^{(lwv)}\hat{\rho}_p$, ${}^{(lwv)}\hat{\varrho}_p$ are used to represent the estimation of parameters ${}^{(lwv)}\rho_p$, ${}^{(lwv)}\varrho_p$.*

According to the definition of the error vector (11), we get the FO error system as

$$\begin{aligned} {}_0D_t^{\alpha}\{{}^{(lwv)}e_p\} &= \sum_{i=1}^{n} c_{li}\{{}_0D_t^{\alpha}z_i\} - \sum_{j=1}^{m} b_{wj}\{{}_0D_t^{\alpha}y_j\} - \sum_{k=1}^{m} a_{vk}\{{}_0D_t^{\alpha}x_k\} \\ &= \sum_{i=1}^{n} c_{li}\{\boldsymbol{H}_i(z(t))\boldsymbol{\vartheta} + h_i(z(t)) + \Delta h_i(z(t)) + \mu_i(z,t) + {}^{(lwv)}u_p\} \\ &- \sum_{j=1}^{m} b_{wj}\{\boldsymbol{G}_j(y(t))\boldsymbol{\beta} + g_j(y(t)) + \Delta g_j(y(t)) + D_j(y,t)\} \\ &- \sum_{k=1}^{m} a_{vk}\{\boldsymbol{F}_k(x(t))\boldsymbol{\theta} + f_k(x(t)) + \Delta f_k(x(t)) + \mathrm{d_k}(x,t)\}. \end{aligned} \tag{24}$$

The errors of unknown parameters $\boldsymbol{\theta}, \boldsymbol{\beta}, \boldsymbol{\vartheta}$ have been defined in (14). For convenience, we define error of unknown constants ${}^{(lwv)}\rho_p$, ${}^{(lwv)}\varrho_p$ as ${}^{(lwv)}\tilde{\rho}_p = {}^{(lwv)}\hat{\rho}_p - {}^{(lwv)}\rho_p$, ${}^{(lwv)}\tilde{\varrho}_p = {}^{(lwv)}\hat{\varrho}_p - {}^{(lwv)}\varrho_p$. Thus, the sliding mode surface is designed as ${}^{(lwv)}s_p =$

$\lambda\{^{(lwv)}e_p\}$. We can get the following multi-switching adaptive controller (MSAC) (25) and multi-switching adaptive updating laws (MSAUL) (28):

$$\begin{aligned}\sum_{i=1}^{n} c_{li}\{^{(lwv)}u_p\} = &-\sum_{i=1}^{n} c_{li}h_i + \sum_{j=1}^{m} b_{wj}g_j + \sum_{k=1}^{m} a_{vk}f_k + \sum_{k=1}^{m} a_{vk}\boldsymbol{F}_k(x(t))\hat{\boldsymbol{\theta}} \\ &+ \sum_{j=1}^{m} b_{wj}\boldsymbol{G}_j(y(t))\hat{\boldsymbol{\beta}} - \sum_{i=1}^{n} c_{li}\boldsymbol{H}_i(z(t))\hat{\boldsymbol{\vartheta}} - (^{(lwv)}\hat{\rho}_p + {}^{(lwv)}\hat{\varrho}_p)sgn(^{(lwv)}s_p) \\ &- k_1 sgn(^{(lwv)}s_p),\end{aligned} \tag{25}$$

where λ, k_1 are constants. Substituting (25) into Equation (24), we obtain

$$\begin{aligned}{}_0D_t^{\alpha}\{^{(lwv)}e_p\} = &\sum_{i=1}^{n} c_{li}\{-\boldsymbol{H}_i(z(t))\tilde{\boldsymbol{\vartheta}} + \Delta h_i(z(t)) + \mu_i(z,t)\} \\ &+ \sum_{j=1}^{m} b_{wj}\{\boldsymbol{G}_j(y(t))\tilde{\boldsymbol{\beta}} - \Delta g_j(y(t)) - D_j(y,t)\} \\ &+ \sum_{k=1}^{m} a_{vk}\{\boldsymbol{F}_k(x(t))\tilde{\boldsymbol{\theta}} - \Delta f_k(x(t)) - \mathrm{d}_k(x,t)\} \\ &- (^{(lwv)}\hat{\rho}_p + {}^{(lwv)}\hat{\varrho}_p)sgn(^{(lwv)}s_p) - k_1 sgn(^{(lwv)}s_p).\end{aligned} \tag{26}$$

Therefore, a column vector representing the general form of the error system (26), whose elements are chosen arbitrarily form $^{(lwv)}e$ (i.e., when $l = 2, w = 3, v = 1$, an error mode is generated $^{(231)}e$), can be obtained the following form:

$$\begin{aligned}{}_0D_t^{\alpha}\boldsymbol{e}(t) = &-C\boldsymbol{H}(z(t))\tilde{\boldsymbol{\vartheta}} + B\boldsymbol{G}(y(t))\tilde{\boldsymbol{\beta}} + A\boldsymbol{F}(x(t))\tilde{\boldsymbol{\theta}} + C\Delta\boldsymbol{h}(z(t)) - B\Delta\boldsymbol{g}(y(t)) \\ &- A\Delta\boldsymbol{f}(x(t)) + C\boldsymbol{\mu}(z,t) - B\boldsymbol{D}(y,t) - A\boldsymbol{d}(x,t) - (\boldsymbol{\rho} + \boldsymbol{\varrho}) \circ sgn(\boldsymbol{s}) - k_1 sgn(\boldsymbol{s}).\end{aligned} \tag{27}$$

where $\circ$ represents the Hadamard product operator, $\boldsymbol{\rho} = (^{(ijk)}\rho_1, {}^{(ijk)}\rho_2, \cdots, {}^{(ijk)}\rho_p)$, $\boldsymbol{\varrho} = (^{(ijk)}\varrho_1, {}^{(ijk)}\varrho_2, \cdots, {}^{(ijk)}\varrho_p)$, the non-diagonal matrices $A = (a_{vk})_{n\times m}$, $B = (b_{wj})_{n\times m}$, $C = (c_{li})_{n\times n}, C \neq 0$.

The MSAUL with regard to unknown parameters $\boldsymbol{\theta}, \boldsymbol{\beta}, \boldsymbol{\vartheta}, {}^{(lwv)}\rho_p, {}^{(lwv)}\varrho_p$ are selected as

$$\begin{aligned}&{}_0D_t^{\alpha}\hat{\boldsymbol{\theta}} = -\lambda\boldsymbol{F}^T(x(t))A^T\boldsymbol{s} - \varphi_1 sgn(\tilde{\boldsymbol{\theta}})|(\tilde{\boldsymbol{\theta}})|^w, \\ &{}_0D_t^{\alpha}\hat{\boldsymbol{\beta}} = -\lambda\boldsymbol{G}^T(y(t))B^T\boldsymbol{s} - \varphi_2 sgn(\tilde{\boldsymbol{\beta}})|(\tilde{\boldsymbol{\beta}})|^w, \\ &{}_0D_t^{\alpha}\hat{\boldsymbol{\vartheta}} = \lambda\boldsymbol{H}^T(z(t))C^T\boldsymbol{s} - \varphi_3 sgn(\tilde{\boldsymbol{\vartheta}})|(\tilde{\boldsymbol{\vartheta}})|^w, \\ &{}_0D_t^{\alpha}\{^{(lwv)}\hat{\rho}_p\} = m_1\lambda|^{(lwv)}s_p|, \\ &{}_0D_t^{\alpha}\{^{(lwv)}\hat{\varrho}_p\} = m_2\lambda|^{(lwv)}s_p|,\end{aligned} \tag{28}$$

where $m_1, m_2, \varphi_1, \varphi_2, \varphi_3, w$ are positive constants and a column vector representing the general form of sliding mode surface $^{(ijk)}s_p = \lambda\{^{(ijk)}e_p\}$ can be obtained as $\boldsymbol{s} = \lambda\boldsymbol{e}$, $p = 1, 2, \cdots, n$.

Theorem 3. *For any given initial conditions $\boldsymbol{x}(0), \boldsymbol{y}(0), \boldsymbol{z}(0)$, if the Assumption 2 (2) is held, the synchronization error system (11) will achieve the multi-switching sliding mode combination synchronization (MSSMCS) via the multi-switching adaptive controller (MSAC) (25) and multi-switching adaptive updating laws (MSAUL) (28).*

Proof. Adopting the Lyapunov function as:

$$V = \frac{1}{2}\boldsymbol{s}^T\boldsymbol{s} + \frac{1}{2}\tilde{\boldsymbol{\theta}}^T\boldsymbol{\theta} + \frac{1}{2}\tilde{\boldsymbol{\beta}}^T\boldsymbol{\beta} + \frac{1}{2}\tilde{\boldsymbol{\vartheta}}^T\boldsymbol{\vartheta} + \frac{1}{2m_1}\sum_{p=1}^{n}\{^{(lwv)}\tilde{\rho}_p^T\}\{^{(lwv)}\tilde{\rho_p}\} + \frac{1}{2m_2}\sum_{p=1}^{n}\{^{(lwv)}\tilde{\varrho}_p^T\}\{^{(lwv)}\tilde{\varrho_p}\} \tag{29}$$

Taking the α derivative

$$_0D_t^\alpha V(t,\boldsymbol{x}(t)) \leq \boldsymbol{s}^T{}_0D_t^\alpha\boldsymbol{s} + \tilde{\boldsymbol{\theta}}^T{}_0D_t^\alpha\hat{\boldsymbol{\theta}} + \tilde{\boldsymbol{\beta}}^T{}_0D_t^\alpha\hat{\boldsymbol{\beta}} + \tilde{\boldsymbol{\vartheta}}^T{}_0D_t^\alpha\hat{\boldsymbol{\vartheta}} + \frac{1}{m_1}\sum_{p=1}^{n}\{^{(lwv)}\tilde{\rho}_p^T\}_0D_t^\alpha\{^{(lwv)}\hat{\rho}_p\} + \frac{1}{m_2}\sum_{p=1}^{n}\{^{(lwv)}\tilde{\varrho}_p^T\}_0D_t^\alpha\{^{(lwv)}\hat{\varrho}_p\}. \tag{30}$$

Substituting the (27) and MSAUL (28) into Equation (30), then, the rest of the proof process is similar to Theorem 2. Finally, one can obtain $_0D_t^\alpha V(t,\boldsymbol{x}(t)) \leq -k_1\lambda\|\boldsymbol{s}\|$.

It is obvious that $V(t)$ is positive-definite and $_0D_t^\alpha V(t,\boldsymbol{x}(t))$ is negative semi-definite. Based on Barbalat's lemma [58], $\lim_{t\to\infty}{}_0D_t^\alpha V(t,\boldsymbol{x}(t)) = 0$ is obtained. We have $\lim_{t\to\infty}\|\boldsymbol{s}\| = 0$. Then, the trajectory of the error system is driven onto the predefined sliding surface, i.e., we can say that the MSSMCS of the drive systems (6), (7) and response system (8) is accomplished in terms of $m \neq n$. □

The following corollaries are successfully analyzed from Theorem 3 and their proofs are omitted here. By the way, the Theorem 2 has the same theory, we are not going to describe it.

Corollary 1. *If the matrices $A \neq 0, B = 0, C \neq 0$, then the drive system (6) achieves the MSSMCS with the response system (8) providing the following controller,*

$$\sum_{i=1}^{n}c_{li}\{^{(lwv)}u_p\} = -\sum_{i=1}^{n}c_{li}h_i + \sum_{k=1}^{m}a_{vk}f_k + \sum_{k=1}^{m}a_{vk}\boldsymbol{F}_k(x(t))\hat{\boldsymbol{\theta}} - \sum_{i=1}^{n}c_{li}\boldsymbol{H}_i(z(t))\hat{\boldsymbol{\vartheta}} - (^{(lwv)}\hat{\rho}_p + {}^{(lwv)}\hat{\varrho}_p)sgn(^{(lwv)}s_p) - k_1 sgn(^{(lwv)}s_p).$$

In addition to the adaptive updating laws,

$$\begin{aligned}
{}_0D_t^\alpha\hat{\boldsymbol{\theta}} &= -\boldsymbol{F}^T(x(t))A^T\boldsymbol{s} - \varphi_1 sgn(\tilde{\boldsymbol{\theta}})|(\tilde{\boldsymbol{\theta}})|^w,\\
{}_0D_t^\alpha\hat{\boldsymbol{\vartheta}} &= \boldsymbol{H}^T(z(t))C^T\boldsymbol{s} - \varphi_3 sgn(\tilde{\boldsymbol{\vartheta}})|(\tilde{\boldsymbol{\vartheta}})|^w,\\
{}_0D_t^\alpha\{^{(lwv)}\hat{\rho}_p\} &= m_1\lambda|^{(lwv)}s_p(t)|,\\
{}_0D_t^\alpha\{^{(lwv)}\hat{\varrho}_p\} &= m_2\lambda|^{(lwv)}s_p(t)|,
\end{aligned}$$

Corollary 2. *If the matrices $A = 0, B \neq 0, C \neq 0$, then the drive system (7) achieves the MSSMCS with the response system (8) providing the following controller,*

$$\sum_{i=1}^{n}c_{li}\{^{(lwv)}u_p\} = -\sum_{i=1}^{n}c_{li}h_i + \sum_{j=1}^{m}b_{wj}g_j + \sum_{j=1}^{m}b_{wj}\boldsymbol{G}_j(y(t))\hat{\boldsymbol{\beta}} - \sum_{i=1}^{n}c_{li}\boldsymbol{H}_i(z(t))\hat{\boldsymbol{\vartheta}} - (^{(lwv)}\hat{\rho}_p + {}^{(lwv)}\hat{\varrho}_p)sgn(^{(lwv)}s_p) - k_1 sgn(^{(lwv)}s_p).$$

In addition to the adaptive updating laws,

$$
\begin{aligned}
{}_0D_t^{\alpha}\hat{\boldsymbol{\beta}} &= -\boldsymbol{G}^T(y(t))B^T\boldsymbol{s} - \varphi_2 sgn(\tilde{\boldsymbol{\beta}})|(\tilde{\boldsymbol{\beta}})|^{w},\\
{}_0D_t^{\alpha}\hat{\boldsymbol{\vartheta}} &= \boldsymbol{H}^T(z(t))C^T\boldsymbol{s} - \varphi_3 sgn(\tilde{\boldsymbol{\vartheta}})|(\tilde{\boldsymbol{\vartheta}})|^{w},\\
{}_0D_t^{\alpha}\{{}^{(lwv)}\hat{\rho}_p\} &= m_1\lambda|{}^{(lwv)}s_p(t)|,\\
{}_0D_t^{\alpha}\{{}^{(lwv)}\hat{\varrho}_p\} &= m_2\lambda|{}^{(lwv)}s_p(t)|,
\end{aligned}
$$

Corollary 3. *If the matrices $A = 0, B = 0, C \neq 0$, then the equilibrium point $(0,0,0,0)$ of the response systems (8) is asymptotically stable provided the following controller,*

$$
\begin{aligned}
\sum_{i=1}^{n} c_{li}\{{}^{(lwv)}u_p\} = &-\sum_{i=1}^{n} c_{li}h_i - \sum_{i=1}^{n} c_{li}\boldsymbol{H}_i(z(t))\hat{\boldsymbol{\vartheta}}\\
&- ({}^{(lwv)}\hat{\rho}_p + {}^{(lwv)}\hat{\varrho}_p)sgn({}^{(lwv)}s_p) - k_1 sgn({}^{(lwv)}s_p),
\end{aligned}
$$

In addition to the adaptive updating laws,

$$
\begin{aligned}
{}_0D_t^{\alpha}\hat{\boldsymbol{\vartheta}} &= \boldsymbol{H}^T(z(t))C^T\boldsymbol{s} - \varphi_3 sgn(\tilde{\boldsymbol{\vartheta}})|(\tilde{\boldsymbol{\vartheta}})|^{w},\\
{}_0D_t^{\alpha}\{{}^{(lwv)}\hat{\rho}_p\} &= m_1\lambda|{}^{(lwv)}s_p(t)|,\\
{}_0D_t^{\alpha}\{{}^{(lwv)}\hat{\varrho}_p\} &= m_2\lambda|{}^{(lwv)}s_p(t)|,
\end{aligned}
$$

6. Numerical Simulation

This section mainly demonstrates the reliability and validity of the suggested multi-switching sliding mode combination synchronization scheme. For the D-R systems (6)–(8) with the same dimensions, we selected two error states to elaborate the method, namely, $i \neq j \neq k$ and $i \neq j = k$. For the D-R systems (6)–(8) with different dimensions, we selected $l \neq w \neq v$ and $l \neq w = v$. In each case, we give the specific forms of controllers and parameter adapting laws via the specific FO hyper-chaotic or chaotic systems.

6.1. Numerical Simulations for FO Chaotic System with Same Dimension

As an example, we choose FO hyper-chaotic Lorenz, Chen systems as the drive systems, and the FO hyper-chaotic Lü system as the response system. Adding SD to the D-R systems, we obtain

$$
\begin{pmatrix} {}_0D_t^{\alpha}x_1\\ {}_0D_t^{\alpha}x_2\\ {}_0D_t^{\alpha}x_3\\ {}_0D_t^{\alpha}x_4 \end{pmatrix} = \begin{pmatrix} x_2-x_1 & 0 & 0 & 0\\ 0 & x_1 & 0 & 0\\ 0 & 0 & -x_3 & 0\\ 0 & 0 & 0 & x_4 \end{pmatrix}\begin{pmatrix} a_1\\ b_1\\ c_1\\ d_1 \end{pmatrix} + \begin{pmatrix} x_4+\Delta f_1\\ -x_1x_3-x_2+\Delta f_2\\ x_1x_2+\Delta f_3\\ -x_2x_3+\Delta f_4 \end{pmatrix} + \begin{pmatrix} \mathrm{d}_1\\ \mathrm{d}_2\\ \mathrm{d}_3\\ \mathrm{d}_4 \end{pmatrix}, \tag{31}
$$

$$
\begin{pmatrix} {}_0D_t^{\alpha}y_1\\ {}_0D_t^{\alpha}y_2\\ {}_0D_t^{\alpha}y_3\\ {}_0D_t^{\alpha}y_4 \end{pmatrix} = \begin{pmatrix} y_2-y_1 & 0 & 0 & 0 & 0\\ 0 & 0 & y_2 & y_1 & 0\\ 0 & -y_3 & 0 & 0 & 0\\ 0 & 0 & 0 & 0 & y_4 \end{pmatrix}\begin{pmatrix} a_2\\ b_2\\ c_2\\ d_2\\ \mathrm{r} \end{pmatrix} + \begin{pmatrix} y_4+\Delta g_1\\ -y_1y_3+\Delta g_2\\ y_1y_2+\Delta g_3\\ y_2y_3+\Delta g_4 \end{pmatrix} + \begin{pmatrix} D_1\\ D_2\\ D_3\\ D_4 \end{pmatrix}, \tag{32}
$$

$$
\begin{pmatrix} {}_0D_t^{\alpha}z_1\\ {}_0D_t^{\alpha}z_2\\ {}_0D_t^{\alpha}z_3\\ {}_0D_t^{\alpha}z_4 \end{pmatrix} = \begin{pmatrix} z_2-z_1 & 0 & 0 & 0\\ 0 & z_2 & 0 & 0\\ 0 & 0 & -z_3 & 0\\ 0 & 0 & 0 & z_4 \end{pmatrix}\begin{pmatrix} a_3\\ b_3\\ c_3\\ d_3 \end{pmatrix} + \begin{pmatrix} z_4+\Delta h_1\\ -z_1z_3+\Delta h_2\\ z_1z_2+\Delta h_3\\ z_1z_3+\Delta h_4 \end{pmatrix} + \begin{pmatrix} \mu_1+u_1\\ \mu_2+u_2\\ \mu_3+u_3\\ \mu_4+u_4 \end{pmatrix}. \tag{33}
$$

Choosing the parameters are $a_1 = 10, b_1 = 28, c_1 = 8/3, d_1 = -1, a_2 = 35, b_2 = 3, c_2 = 12, d_2 = 7, \mathrm{r} = 0.5, a_3 = 36, b_3 = 20, c_3 = 3, d_3 = 0.5$. The initial conditions take as $x(0) = (2,-2,1,1), y(0) = (1,1,2,2), z(0) = (-20,3,1,3,)$. When $\boldsymbol{\Delta}g = 0$, $\boldsymbol{\Delta}f = 0$, $\boldsymbol{\Delta}h = 0$,

$\boldsymbol{d}(t) = 0$, $\boldsymbol{D}(t) = 0$, $\boldsymbol{\mu}(t) = 0$ and $\alpha = 0.97$, we can obtain the attractor graphs of the FO hyper-chaotic Lorenz, Chen, and Lü system using the FO prediction-correction method which are presented in Figure 1.

In relation to (12), the multi-switching error state modes between the drive systems (31), (32) and the response system (33) are listed for $i, j, k = 1, 2, 3, 4$:

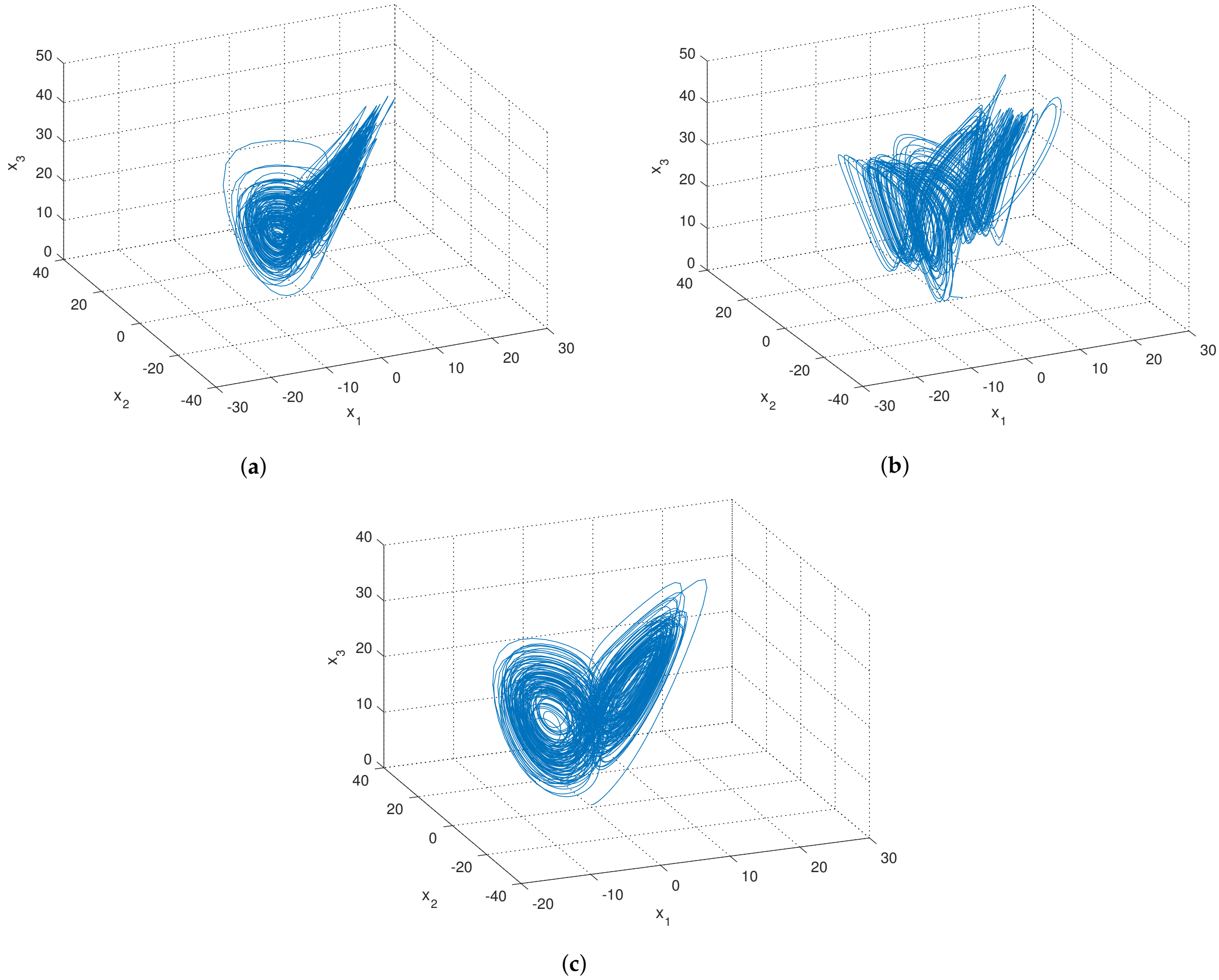

Figure 1. The 3D phase plots of FO hyper-chaotic Lorenz, Chen, Lü systems indicating in sub-pictures (**a**–**c**), respectively.

$$Switch{-}1 : i \neq j \neq k \begin{cases} {}^{(123)}e_1, & {}^{(132)}e_2, & {}^{(124)}e_3, & {}^{(142)}e_4, & {}^{(134)}e_5, & {}^{(143)}e_6, \\ {}^{(213)}e_7, & {}^{(231)}e_8, & {}^{(214)}e_9, & {}^{(241)}e_{10}, & {}^{(234)}e_{11}, & {}^{(243)}e_{12}, \\ {}^{(321)}e_{13}, & {}^{(312)}e_{14}, & {}^{(324)}e_{15}, & {}^{(314)}e_{16}, & {}^{(341)}e_{17}, & {}^{(342)}e_{18}, \\ {}^{(412)}e_{19}, & {}^{(421)}e_{20}, & {}^{(413)}e_{21}, & {}^{(423)}e_{22}, & {}^{(432)}e_{23}, & {}^{(431)}e_{24}. \end{cases}$$

$$Switch{-}2 : i \neq j = k \begin{cases} {}^{(122)}e_{25}, & {}^{(133)}e_{26}, & {}^{(144)}e_{27}, & {}^{(211)}e_{28}, & {}^{(233)}e_{29}, & {}^{(244)}e_{30}, \\ {}^{(311)}e_{31}, & {}^{(322)}e_{32}, & {}^{(344)}e_{33}, & {}^{(411)}e_{34}, & {}^{(422)}e_{35}, & {}^{(433)}e_{36}. \end{cases}$$

$$Switch{-}3 : i = j \neq k \begin{cases} {}^{(112)}e_{37}, & {}^{(113)}e_{38}, & {}^{(114)}e_{39}, & {}^{(221)}e_{40}, & {}^{(223)}e_{41}, & {}^{(224)}e_{42}, \\ {}^{(331)}e_{43}, & {}^{(332)}e_{44}, & {}^{(334)}e_{45}, & {}^{(441)}e_{46}, & {}^{(442)}e_{47}, & {}^{(443)}e_{48}. \end{cases}$$

$$Switch{-}4 : i = k \neq j \begin{cases} {}^{(121)}e_{49}, & {}^{(131)}e_{50}, & {}^{(141)}e_{51}, & {}^{(212)}e_{52}, & {}^{(232)}e_{53}, & {}^{(242)}e_{54}, \\ {}^{(313)}e_{55}, & {}^{(323)}e_{56}, & {}^{(343)}e_{57}, & {}^{(414)}e_{58}, & {}^{(424)}e_{59}, & {}^{(434)}e_{60}. \end{cases}$$

$$Switch{-}5: i=k=j\begin{cases} {}^{(111)}e_{61}, & {}^{(222)}e_{62}, \\ {}^{(333)}e_{63}, & {}^{(444)}e_{64}. \end{cases}$$

In this section, we arbitrarily select the appropriate switching error variables for the situation of Switch-1 ($i \neq j \neq k$) from above, namely, $\boldsymbol{e} = ({}^{(124)}e_3, {}^{(243)}e_{12}, {}^{(312)}e_{14}, {}^{(431)}e_{24})^T$; For Switch-2 ($i \neq j = k$), we arbitrarily select $\boldsymbol{e} = ({}^{(122)}e_{25}, {}^{(244)}e_{30}, {}^{(311)}e_{31}, {}^{(433)}e_{36})^T$. Thus, the following two switching modes for numerical simulation are obtained:

$$Switch{-}1: \begin{pmatrix} {}^{(124)}e_3 = c_{11}z_1 - (b_{22}y_2 + a_{44}x_4) \\ {}^{(243)}e_{12} = c_{22}z_2 - (b_{44}y_4 + a_{33}x_3) \\ {}^{(312)}e_{14} = c_{33}z_3 - (b_{11}y_1 + a_{22}x_2) \\ {}^{(431)}e_{24} = c_{44}z_4 - (b_{33}y_3 + a_{11}x_1) \end{pmatrix}, \tag{34}$$

$$Switch{-}2: \begin{pmatrix} {}^{(122)}e_{25} = c_{11}z_1 - (b_{22}y_2 + a_{22}x_2) \\ {}^{(244)}e_{30} = c_{22}z_2 - (b_{44}y_4 + a_{44}x_4) \\ {}^{(311)}e_{31} = c_{33}z_3 - (b_{11}y_1 + a_{11}x_1) \\ {}^{(433)}e_{36} = c_{44}z_4 - (b_{33}y_3 + a_{33}x_3) \end{pmatrix}. \tag{35}$$

In order to confirm the robustness and reliability of the investigated MSAC (15) and MSAUL (18), the nonlinear uncertainties and external disturbances are selected as follows:

$$\begin{aligned} \boldsymbol{d}(\boldsymbol{x}(t)) &= (-0.1cos(t), -0.2cos(2t), 0.3sin(3t), 0.4sin(4t))^T, \\ \boldsymbol{D}(\boldsymbol{y}(t)) &= (-0.1sin(t), -0.2sin(2t), 0.3cos(3t), 0.4cos(4t))^T, \\ \boldsymbol{\mu}(\boldsymbol{z}(t)) &= (0.1cos(5t), 0.2cos(6t), 0.3sin(7t), 0.4sin(8t))^T, \\ \Delta\boldsymbol{f}(\boldsymbol{x}(t)) &= (0.1cos(2tx_1), 0.2cos(2tx_2), 0.3sin(2tx_3), 0.4sin(2tx_4))^T, \\ \Delta\boldsymbol{g}(\boldsymbol{y}(t)) &= (0.1sin(2\pi t), 0.2sin(sgn(y_2)), 0.3cos(2\pi y_3), 0.4cos(4tx_8))^T, \\ \Delta\boldsymbol{h}(\boldsymbol{z}(t)) &= (0.1sin(2tsgn(z_1)), 0.2sin(2tsgn(z_2)), 0.3sin(3t), 0.4sin(4t))^T. \end{aligned} \tag{36}$$

6.1.1. Switch-1

It follows from Switch-1 (34) that the FO error dynamic systems are expressed as:

$$\begin{aligned} {}_0D_t^\alpha\{{}^{(124)}e_3\} =& c_{11}\{{}_0D_t^\alpha z_1\} - b_{22}\{{}_0D_t^\alpha y_2\} - a_{44}\{{}_0D_t^\alpha x_4\} \\ =& c_{11}\{(z_2 - z_1)a_3 + z_4 + \Delta h_1 + \mu_1 +^{(124)} u_3\} \\ & -b_{22}\{y_2c_2 + d_2y_1 - y_1y_3 + \Delta g_2 + D_2\} \\ & -a_{44}\{x_4d_1 - x_2x_3 + \Delta f_4 + \mathrm{d}_4\}, \\ {}_0D_t^\alpha\{{}^{(243)}e_{12}\} =& c_{22}\{{}_0D_t^\alpha z_2\} - b_{44}\{{}_0D_t^\alpha y_4\} - a_{33}\{{}_0D_t^\alpha x_3\} \\ =& c_{22}\{z_2b_3 - z_1z_3 + \Delta h_2 + \mu_2 +^{(243)} u_{12}\} \\ & -b_{44}\{y_4\mathrm{r} + y_2y_3 + \Delta g_4 + D_4\} \\ & -a_{33}\{-x_3c_1 + x_1x_2 + \Delta f_3 + \mathrm{d}_3\}, \\ {}_0D_t^\alpha\{{}^{(312)}e_{14}\} =& c_{33}\{{}_0D_t^\alpha z_3\} - b_{11}\{{}_0D_t^\alpha y_1\} - a_{22}\{{}_0D_t^\alpha x_2\} \\ =& c_{33}\{-z_3c_3 + z_1z_2 + \Delta h_3 + \mu_3 +^{(312)} u_{14}\} \\ & -b_{11}\{(y_2 - y_1)a_2 + y_4 + \Delta g_1 + D_1\} \\ & -a_{22}\{x_1b_1 - x_1x_3 - x_2 + \Delta f_2 + \mathrm{d}_2\}, \\ {}_0D_t^\alpha\{{}^{(431)}e_{24}\} =& c_{44}\{{}_0D_t^\alpha z_4\} - b_{33}\{{}_0D_t^\alpha y_3\} - a_{11}\{{}_0D_t^\alpha x_1\} \\ =& c_{44}\{z_4d_3 + z_1z_3 + \Delta h_4 + \mu_4 +^{(431)} u_{24}\} \\ & -b_{33}\{(-y_3b_2 + y_1y_2 + \Delta g_3 + D_3\} \\ & -a_{11}\{(x_2 - x_1)a_1 + x_4 + \Delta f_1 + \mathrm{d}_1\}. \end{aligned} \tag{37}$$

For the convenience, let us denote ${}^{(124)}e_3 = E_1$, ${}^{(243)}e_{12} = E_2$, ${}^{(312)}e_{14} = E_3$, ${}^{(431)}e_{24} = E_4$, the sliding mode surfaces ${}^{(124)}s_3 = S_1 = \lambda E_1$, ${}^{(243)}s_{12} = S_2 = \lambda E_2$, ${}^{(312)}s_{14} = S_3 = \lambda E_3$, ${}^{(431)}s_{24} = S_4 = \lambda E_4$, the controllers ${}^{(124)}u_3 = U_1$, ${}^{(243)}u_{12} = U_2$, ${}^{(312)}u_{14} = U_3$, ${}^{(431)}u_{24} = U_4$, the upper bound values of stochastic disturbances ${}^{(124)}r_3 = R_1$, ${}^{(243)}r_{12} = R_2$, ${}^{(312)}r_{14} = R_3$, ${}^{(431)}r_{24} = R_4$, ${}^{(124)}q_3 = Q_1$, ${}^{(243)}q_{12} = Q_2$, ${}^{(312)}q_{14} = Q_3$, ${}^{(431)}q_{24} = Q_4$. It follows from the forms of MSAC (15) and MSAUL (18) that the controllers are designed as follows:

$$
\begin{aligned}
U_1 =& - z_4 - (z_2 - z_1)\hat{a}_3 + \frac{b_{22}}{c_{11}}(-y_1y_3 + y_2\hat{c}_2 + \hat{d}_2y_1) + \frac{a_{44}}{c_{11}}(-x_2x_3 + x_4\hat{d}_1) \\
& -(\hat{R}_1 + \hat{Q}_1)sgn(S_1) - k_1 sgn(S_1), \\
U_2 =& z_1z_3 - z_2\hat{b}_3 + \frac{b_{44}}{c_{22}}(y_2y_3 + y_4\hat{\mathrm{r}}) + \frac{a_{33}}{c_{22}}(x_2x_1 - x_3\hat{c}_1) \\
& -(\hat{R}_2 + \hat{Q}_2)sgn(S_2) - k_1 sgn(S_2), \\
U_3 =& - z_1z_2 + z_3\hat{c}_3 + \frac{b_{11}}{c_{33}}(y_4 + (y_2 - y_1)\hat{a}_2) + \frac{a_{22}}{c_{33}}(x_1x_3 + x_2 + x_1\hat{b}_1) \\
& -(\hat{R}_3 + \hat{Q}_3)sgn(S_3) - k_1 sgn(S_3), \\
U_4 =& - z_1z_3 - z_4\hat{d}_3 + \frac{b_{33}}{c_{44}}(y_1y_2 - y_3\hat{b}_2) + \frac{a_{11}}{c_{44}}(x_4 + (x_2 - x_1)\hat{a}_1) \\
& -(\hat{R}_4 + \hat{Q}_4)sgn(S_4) - k_1 sgn(S_4).
\end{aligned}
\tag{38}
$$

and the parameters updating laws are designed as follows:

$$
\begin{aligned}
&{}_0D_t^\alpha \hat{a}_1 = -\lambda a_{11}(x_2 - x_1)S_4 - \varphi_1 sgn(\tilde{a}_1)|\tilde{a}_1|^\omega, \quad {}_0D_t^\alpha \hat{b}_1 = -\lambda a_{22}x_1S_3 - \varphi_1 sgn(\tilde{b}_1)|\tilde{b}_1|^\omega, \\
&{}_0D_t^\alpha \hat{c}_1 = \lambda a_{33}x_3S_2 - \varphi_1 sgn(\tilde{c}_1)|\tilde{c}_1|^\omega, \quad {}_0D_t^\alpha \hat{d}_1 = -\lambda a_{44}x_4S_1 - \varphi_1 sgn(\tilde{d}_1)|\tilde{d}_1|^\omega, \\
&{}_0D_t^\alpha \hat{a}_2 = -\lambda b_{11}(y_2 - y_1)S_3 - \varphi_2 sgn(\tilde{a}_2)|\tilde{a}_2|^\omega, \quad {}_0D_t^\alpha \hat{b}_2 = \lambda b_{33}y_3S_4 - \varphi_2 sgn(\tilde{b}_2)|\tilde{b}_2|^\omega, \\
&{}_0D_t^\alpha \hat{c}_2 = -\lambda b_{22}y_2S_1 - \varphi_2 sgn(\tilde{c}_2)|\tilde{c}_2|^\omega, \quad {}_0D_t^\alpha \hat{d}_2 = -\lambda b_{22}y_1S_1 - \varphi_2 sgn(\tilde{d}_2)|\tilde{d}_2|^\omega, \\
&{}_0D_t^\alpha \hat{\mathrm{r}} = -\lambda b_{44}y_4S_2 - \varphi_2 sgn(\tilde{r})|\tilde{r}|^\omega, \quad {}_0D_t^\alpha \hat{a}_3 = \lambda c_{11}(z_2 - z_1)S_1 - \varphi_3 sgn(\tilde{a}_3)|\tilde{a}_3|^\omega, \\
&{}_0D_t^\alpha \hat{b}_3 = \lambda c_{22}z_2S_2 - \varphi_3 sgn(\tilde{b}_3)|\tilde{b}_3|^\omega, \quad {}_0D_t^\alpha \hat{c}_3 = -\lambda c_{33}z_3S_3 - \varphi_3 sgn(\tilde{c}_3)|\tilde{c}_3|^\omega, \\
&{}_0D_t^\alpha \hat{d}_3 = \lambda c_{44}z_4S_4 - \varphi_3 sgn(\tilde{d}_3)|\tilde{d}_3|^\omega, \quad {}_0D_t^\alpha \hat{R}_1 = m_1\lambda|S_1|, \quad {}_0D_t^\alpha \hat{R}_2 = m_1\lambda|S_1|, \\
&{}_0D_t^\alpha \hat{R}_3 = m_1\lambda|S_3|, \quad {}_0D_t^\alpha \hat{R}_4 = m_1\lambda|S_4|, \quad {}_0D_t^\alpha \hat{Q}_1 = m_1\lambda|S_1|, \\
&{}_0D_t^\alpha \hat{Q}_2 = m_2\lambda|S_2|, \quad {}_0D_t^\alpha \hat{Q}_3 = m_2\lambda|S_3|, \quad {}_0D_t^\alpha \hat{Q}_4 = m_2\lambda|S_4|.
\end{aligned}
\tag{39}
$$

Theorem 4. *For any given initial conditions $\boldsymbol{x}(0), \boldsymbol{y}(0), \boldsymbol{z}(0)$ of D-R systems (31)–(33), if the Assumption 1 (13) is held, the synchronization error system (37) will achieve the multi-switching sliding mode combination synchronization (MSSMCS) via the multi-switching adaptive controller (MSAC) (38) and multi-switching adaptive updating laws (MSAUL) (39).*

Proof. Adopting the Lyapunov function as:

$$
V = \frac{1}{2}\sum_{p=1}^{4} S_p^2 + \frac{1}{2}\sum_{i=1}^{3}(\tilde{a}_i^2 + \tilde{b}_i^2 + \tilde{c}_i^2 + \tilde{d}_i^2) + \frac{1}{2}\tilde{\mathrm{r}}^2 + \frac{1}{2m_1}\sum_{p=1}^{4}\tilde{R}_p^2 + \frac{1}{2m_2}\sum_{p=1}^{4}\tilde{Q}_p^2 \tag{40}
$$

The α derivative of (40) yields:

$$
\begin{aligned}
D_t^\alpha V \leq & \sum_{p=1}^{4} S_p\{D_t^\alpha S_p\} + \sum_{i=1}^{3}\left(\tilde{a}_i\{D_t^\alpha \hat{a}_i\} + \tilde{b}_i\{D_t^\alpha \hat{b}_i\} + \tilde{c}_i\{D_t^\alpha \hat{c}_i\} + \tilde{d}_i\{D_t^\alpha \hat{d}_i\}\right) \\
& + \tilde{\mathrm{r}}\{D_t^\alpha \hat{\mathrm{r}}\} + \frac{1}{m_1}\sum_{p=1}^{4}\tilde{R}_p\{D_t^\alpha \hat{R}_p\} + \frac{1}{m_2}\sum_{p=1}^{4}\tilde{Q}_p\{D_t^\alpha \hat{Q}_p\}
\end{aligned}
\tag{41}
$$

Then, substituting the error modes (37), the controllers (38) and the MSAUL (39) into Equation (41), we obtain

$$
\begin{aligned}
D_t^{\alpha}V \leq\ & \lambda S_1\big[c_{11}\{-(z_2-z_1)\tilde{a}_3+\Delta h_1+\mu_1\}-b_{22}\{-y_2\tilde{c}_2-\tilde{d}_2y_1+\Delta g_2+D_2\}\\
&-a_{44}\{-x_4\tilde{d}_1+\Delta f_4+\mathrm{d}_4\}-(\hat{R}_1+\hat{Q}_1)sgn(S_1)-k_1sgn(S_1)\big]\\
&+\lambda S_2\big[c_{22}\{-z_2\tilde{b}_3+\Delta h_2+\mu_2\}-b_{44}\{-y_4\tilde{\mathrm{r}}+\Delta g_4+D_4\}\\
&-a_{33}\{x_3\tilde{c}_1+\Delta f_3+\mathrm{d}_3\}-(\hat{R}_2+\hat{Q}_2)sgn(S_2)-k_1sgn(S_2)\big]\\
&+\lambda S_3\big[c_{33}\{z_3\tilde{c}_3+\Delta h_3+\mu_3\}-b_{11}\{-(y_2-y_1)\tilde{a}_2+\Delta g_1+D_1\}\\
&-a_{22}\{-x_1\tilde{b}_1+\Delta f_2+\mathrm{d}_2\}-(\hat{R}_3+\hat{Q}_3)sgn(S_3)-k_1sgn(S_3)\big]\\
&+\lambda S_4\big[c_{44}\{-z_4\tilde{d}_3+\Delta h_4+\mu_4\}-b_{33}\{y_3\tilde{b}_2+\Delta g_3+D_3\}\\
&-a_{11}\{-(x_2-x_1)\tilde{a}_1+\Delta f_1+\mathrm{d}_1\}-(\hat{R}_4+\hat{Q}_4)sgn(S_4)-k_1sgn(S_4)\big]\\
&-\lambda S_1\big[(\hat{R}_1+\hat{Q}_1)sgn(S_1)-k_1sgn(S_1)\big]-\lambda S_2\big[(\hat{R}_2+\hat{Q}_2)sgn(S_2)-k_1sgn(S_2)\big]\\
&-\lambda S_3\big[(\hat{R}_3+\hat{Q}_3)sgn(S_3)-k_1sgn(S_3)\big]-\lambda S_4\big[(\hat{R}_4+\hat{Q}_4)sgn(S_4)-k_1sgn(S_4)\big]\\
&+\tilde{a}_1\big[-\lambda a_{11}(x_2-x_1)S_4-\varphi_1sgn(\tilde{a}_1)|\tilde{a}_1|^{\omega}\big]+\tilde{a}_2\big[-\lambda b_{11}(y_2-y_1)S_3-\varphi_2sgn(\tilde{a}_2)|\tilde{a}_2|^{\omega}\big]\\
&+\tilde{a}_3\big[\lambda c_{11}(z_2-z_1)S_1-\varphi_3sgn(\tilde{a}_3)|\tilde{a}_3|^{\omega}\big]+\tilde{b}_1\big[-\lambda a_{22}x_1S_3-\varphi_1sgn(\tilde{b}_1)|\tilde{b}_1|^{\omega}\big]\\
&+\tilde{b}_2\big[\lambda b_{33}y_3S_4-\varphi_2sgn(\tilde{b}_2)|\tilde{b}_2|^{\omega}\big]+\tilde{b}_3\big[\lambda c_{22}z_2S_2-\varphi_3sgn(\tilde{b}_3)|\tilde{b}_3|^{\omega}\big]\\
&+\tilde{c}_1\big[\lambda a_{33}x_3S_2-\varphi_1sgn(\tilde{c}_1)|\tilde{c}_1|^{\omega}\big])+\tilde{c}_2\big[-\lambda b_{22}y_2S_1-\varphi_2sgn(\tilde{c}_2)|\tilde{c}_2|^{\omega}\big]\\
&+\tilde{c}_3\big[-\lambda c_{33}z_3S_3-\varphi_3sgn(\tilde{c}_3)|\tilde{c}_3|^{\omega}\big]+\tilde{d}_1\big[-\lambda a_{44}x_4S_1-\varphi_1sgn(\tilde{d}_1)|\tilde{d}_1|^{\omega}\big]\\
&+\tilde{d}_2\big[-\lambda b_{22}y_1S_1-\varphi_2sgn(\tilde{d}_2)|\tilde{d}_2|^{\omega}\big]+\tilde{d}_3\big[\lambda c_{44}z_4S_4-\varphi_3sgn(\tilde{d}_3)|\tilde{d}_3|^{\omega}\big]\\
&+\tilde{\mathrm{r}}\big[-\lambda b_{44}y_4S_2-\varphi_2sgn(\tilde{\mathrm{r}})|\tilde{\mathrm{r}}|^{\omega}\big]+\lambda\sum_{p=1}^{4}(\tilde{R}_p|S_p|)+\lambda\sum_{p=1}^{4}(\tilde{Q}_p|S_p|) \qquad (42)\\
\leq\ & \lambda|S_1|\big[|c_{11}\Delta h_1-b_{22}\Delta g_2-a_{44}\Delta f_4|+|c_{11}\mu_1-b_{22}D_2--a_{44}\mathrm{d}_4|\big]\\
&+\lambda|S_2|\big[|c_{22}\Delta h_2-b_{44}\Delta g_4-a_{33}\Delta f_3|+|c_{22}\mu_2-b_{44}D_4--a_{33}\mathrm{d}_3|\big]\\
&+\lambda|S_3|\big[|c_{33}\Delta h_3-b_{11}\Delta g_1-a_{22}\Delta f_2|+|c_{33}\mu_3-b_{11}D_1-a_{22}\mathrm{d}_2|\big]\\
&+\lambda|S_4|\big[|c_{44}\Delta h_4-b_{33}\Delta g_3-a_{11}\Delta f_1|+|c_{44}\mu_4-b_{33}D_3-a_{11}\mathrm{d}_1|\big]\\
&-\lambda S_1\big[(\hat{R}_1+\hat{Q}_1)sgn(S_1)-k_1sgn(S_1)\big]-\lambda S_2\big[(\hat{R}_2+\hat{Q}_2)sgn(S_2)-k_1sgn(S_2)\big]\\
&-\lambda S_3\big[(\hat{R}_3+\hat{Q}_3)sgn(S_3)-k_1sgn(S_3)\big]-\lambda S_4\big[(\hat{R}_4+\hat{Q}_4)sgn(S_4)-k_1sgn(S_4)\big]\\
&-\tilde{a}_1\big[\varphi_1sgn(\tilde{a}_1)|\tilde{a}_1|^{\omega}\big]-\tilde{a}_2\big[\varphi_2sgn(\tilde{a}_2)|\tilde{a}_2|^{\omega}\big]-\tilde{a}_3\big[\varphi_3sgn(\tilde{a}_3)|\tilde{a}_3|^{\omega}\big]\\
&-\tilde{b}_1\big[\varphi_1sgn(\tilde{b}_1)|\tilde{b}_1|^{\omega}\big]-\tilde{b}_2\big[\varphi_2sgn(\tilde{b}_2)|\tilde{b}_2|^{\omega}\big]-\tilde{b}_3\big[\varphi_3sgn(\tilde{b}_3)|\tilde{b}_3|^{\omega}\big]\\
&-\tilde{c}_1\big[\varphi_1sgn(\tilde{c}_1)|\tilde{c}_1|^{\omega}\big]-\tilde{c}_2\big[\varphi_2sgn(\tilde{c}_2)|\tilde{c}_2|^{\omega}\big]-\tilde{c}_3\big[\varphi_3sgn(\tilde{c}_3)|\tilde{c}_3|^{\omega}\big]\\
&-\tilde{d}_1\big[\varphi_1sgn(\tilde{d}_1)|\tilde{d}_1|^{\omega}\big]-\tilde{d}_2\big[\varphi_2sgn(\tilde{d}_2)|\tilde{d}_2|^{\omega}\big]-\tilde{d}_3\big[\varphi_3sgn(\tilde{d}_3)|\tilde{d}_3|^{\omega}\big]\\
&-\tilde{\mathrm{r}}\big[\varphi_2sgn(\tilde{\mathrm{r}})|\tilde{\mathrm{r}}|^{\omega}\big]+\lambda\sum_{p=1}^{4}(\tilde{R}_p|S_p|)+\lambda\sum_{p=1}^{4}(\tilde{Q}_p|S_p|).
\end{aligned}
$$

□

Remark 10. *Due to* $^{(124)}r_3 = R_1$, $^{(243)}r_{12} = R_2$, $^{(312)}r_{14} = R_3$, $^{(431)}r_{24} = R_4$, $^{(124)}q_3 = Q_1$, $^{(243)}q_{12} = Q_2$, $^{(312)}q_{14} = Q_3$, $^{(431)}q_{24} = Q_4$, *it follows from Equation (13) that* $R_p, Q_p, p = 1,2,3,4$ *are positive constants. Thus,* $|\hat{R}_p| = \hat{R}_p, |\hat{Q}_p| = \hat{Q}_p, p = 1,2,3,4$.

Using the fact $S_psgn(S_p) = |S_p|$,(p = 1,2,3,4), $\tilde{a}_isgn(\tilde{a}_i) = |\tilde{a}_i|$, $\tilde{b}_isgn(\tilde{b}_i) = |\tilde{b}_i|$, $\tilde{c}_isgn(\tilde{c}_i) = |\tilde{c}_i|$, $\tilde{d}_isgn(\tilde{d}_i) = |\tilde{d}_i|, (i = 1,2,3,4)$, $\tilde{\mathrm{r}}sgn(\tilde{\mathrm{r}}) = |\tilde{\mathrm{r}}|$ and the Assumption 1 (13) to (42) yields:

$$
{}_0D_t^{\alpha}V(t,\boldsymbol{x}(t)) \leq \lambda\sum_{p=1}^{4}\big[|S_p|(|R_p|+|Q_p|)\big]-\lambda\sum_{p=1}^{4}\big[|S_p|(|\hat{R}_p|+|\hat{Q}_p|)\big]
$$

$$
\begin{aligned}
&-\lambda k_1 \sum_{p=1}^{4}(|S_p|) + \lambda \sum_{p=1}^{4}(\tilde{R}_p|S_p|) + \lambda \sum_{p=1}^{4}(\tilde{Q}_p|S_p|) \\
&-\varphi_1(|\tilde{a}_1|^{\omega+1}) - \varphi_2(|\tilde{a}_2|^{\omega+1}) - \varphi_3(|\tilde{a}_3|^{\omega+1}) - \varphi_1(|\tilde{b}_1|^{\omega+1}) \\
&-\varphi_2(|\tilde{b}_2|^{\omega+1}) - \varphi_3(|\tilde{b}_3|^{\omega+1}) - \varphi_1(|\tilde{c}_1|^{\omega+1}) - \varphi_2(|\tilde{c}_2|^{\omega+1}) \\
&-\varphi_3(|\tilde{c}_3|^{\omega+1}) - \varphi_1(|\tilde{d}_1|^{\omega+1}) - \varphi_2(|\tilde{d}_2|^{\omega+1}) - \varphi_3(|\tilde{d}_3|^{\omega+1}) - \varphi_2(|\tilde{\mathrm{r}}|^{\omega+1}) \\
&= -\lambda k_1 \sum_{p=1}^{4}(|S_p|) - \varphi_1(|\tilde{a}_1|^{\omega+1}) - \varphi_2(|\tilde{a}_2|^{\omega+1}) - \varphi_3(|\tilde{a}_3|^{\omega+1}) \\
&-\varphi_1(|\tilde{b}_1|^{\omega+1}) - \varphi_2(|\tilde{b}_2|^{\omega+1}) - \varphi_3(|\tilde{b}_3|^{\omega+1}) - \varphi_1(|\tilde{c}_1|^{\omega+1}) - \varphi_2(|\tilde{c}_2|^{\omega+1}) \\
&-\varphi_3(|\tilde{c}_3|^{\omega+1}) - \varphi_1(|\tilde{d}_1|^{\omega+1}) - \varphi_2(|\tilde{d}_2|^{\omega+1}) - \varphi_3(|\tilde{d}_3|^{\omega+1}) - \varphi_2(|\tilde{\mathrm{r}}|^{\omega+1}) \\
&\leq -\lambda k_1 \sum_{p=1}^{4}(|S_p|).
\end{aligned}
$$

It is obvious that $V(t)$ is positive-definite and ${}_0D_t^{\alpha}V(t,\boldsymbol{x}(t))$ is negative semi-definite. Based on Barbalat's lemma [58], $\lim_{t\to\infty} {}_0D_t^{\alpha}V(t,\boldsymbol{x}(t)) = 0$ is obtained. We have $\lim_{t\to\infty}|S_p| = 0$. Then, the trajectory of the error system is driven onto the predefined sliding surface, i.e., we can say that the MSSMCS of the drive systems (31), (32) and response system (33) is accomplished in terms of $m = n$.

6.1.2. Switch-2

It follows from Switch-2 (35) that the FO error dynamic systems are expressed as:

$$
\begin{aligned}
{}_0D_t^{\alpha}\{{}^{(122)}e_{25}\} =& c_{11}\{{}_0D_t^{\alpha}z_1\} - b_{22}\{{}_0D_t^{\alpha}y_2\} - a_{22}\{{}_0D_t^{\alpha}x_2\} \\
=& c_{11}\{(z_2 - z_1)a_3 + z_4 + \Delta h_1 + \mu_1 +^{(122)} u_{25}\} \\
& - b_{22}\{y_2c_2 + d_2y_1 - y_1y_3 + \Delta g_2 + D_2\} \\
& - a_{22}\{x_1b_1 - x_1x_3 - x_2 + \Delta f_2 + \mathrm{d}_2\} \\
{}_0D_t^{\alpha}\{{}^{(244)}e_{30}\} =& c_{22}\{{}_0D_t^{\alpha}z_2\} - b_{44}\{{}_0D_t^{\alpha}y_4\} - a_{44}\{{}_0D_t^{\alpha}x_4\} \\
=& c_{22}\{z_2b_3 - z_1z_3 + \Delta h_2 + \mu_2 +^{(244)} u_{30}\} \\
& - b_{44}\{y_4\mathrm{r} + y_2y_3 + \Delta g_4 + D_4\} \\
& - a_{44}\{x_4d_1 - x_2x_3 + \Delta f_4 + \mathrm{d}_4\} \\
{}_0D_t^{\alpha}\{{}^{(311)}e_{31}\} =& c_{33}\{{}_0D_t^{\alpha}z_3\} - b_{11}\{{}_0D_t^{\alpha}y_1\} - a_{11}\{{}_0D_t^{\alpha}x_1\} \\
=& c_{33}\{-z_3c_3 + z_1z_2 + \Delta h_3 + \mu_3 +^{(311)} u_{31}\} \\
& - b_{11}\{(y_2 - y_1)a_2 + y_4 + \Delta g_1 + D_1\} \\
& - a_{11}\{(x_2 - x_1)a_1 + x_4 + \Delta f_1 + \mathrm{d}_1\} \\
{}_0D_t^{\alpha}\{{}^{(433)}e_{36}\} =& c_{44}\{{}_0D_t^{\alpha}z_4\} - b_{33}\{{}_0D_t^{\alpha}y_3\} - a_{33}\{{}_0D_t^{\alpha}x_3\} \\
=& c_{44}\{z_4d_3 + z_1z_3 + \Delta h_4 + \mu_4 +^{(433)} u_{36}\} \\
& - b_{33}\{-y_3b_2 + y_1y_2 + \Delta g_3 + D_3\} \\
& - a_{33}\{-x_3c_1 + x_1x_2 + \Delta f_3 + \mathrm{d}_3\}
\end{aligned}
$$

It follows from the forms of MSAC (15) and MSAUL (18) that the controllers are designed as follows:

$$
\begin{aligned}
{}^{(122)}u_{25} =& -z_4 - (z_2 - z_1)\hat{a}_3 + \frac{b_{22}}{c_{11}}(y_1y_3 + y_2\hat{c}_2 + \hat{d}_2y_1) + \frac{a_{22}}{c_{11}}(-x_1x_3 - x_2 + x_1\hat{b}_1) \\
& - ({}^{(122)}\hat{r}_{25} +^{(122)} \hat{q}_{25})sgn({}^{(122)}s_{25}) - k_1 sgn({}^{(122)}s_{25}), \\
{}^{(244)}u_{30} =& z_1z_3 - z_2\hat{b}_3 + \frac{b_{44}}{c_{22}}(y_2y_3 + y_4\hat{\mathrm{r}}) + \frac{a_{44}}{c_{22}}(-x_2x_3 + x_4\hat{d}_1)
\end{aligned}
$$

$$
\begin{aligned}
&-({}^{(244)}\hat{r}_{30}+{}^{(244)}\hat{q}_{30})sgn({}^{(244)}s_{30})-k_1sgn({}^{(244)}s_{30}),\\
{}^{(311)}u_{31}=&-z_1z_2+z_3\hat{c}_3+\frac{b_{11}}{c_{33}}(y_4+(y_2-y_1)\hat{a}_2)+\frac{a_{11}}{c_{33}}(x_4+(x_2-x_1)\hat{a}_1)\\
&-({}^{(311)}\hat{r}_{31}+{}^{(311)}\hat{q}_{31})sgn({}^{(311)}s_{31})-k_1sgn({}^{(311)}s_{31}),\\
{}^{(433)}u_{36}=&-z_1z_3-z_4\hat{d}_3+\frac{b_{33}}{c_{44}}(y_1y_2-y_3\hat{b}_2)+\frac{a_{33}}{c_{44}}(x_1x_2-x_3\hat{c}_1)\\
&-({}^{(433)}\hat{r}_{36}+{}^{(433)}\hat{q}_{36})sgn({}^{(433)}s_{36})-k_1sgn({}^{(433)}s_{36}).
\end{aligned}
$$

and the parameters updating laws are designed as follows:

$$
\begin{array}{ll}
{}_0D_t^\alpha\hat{a}_1=-\lambda a_{11}(x_2-x_1)({}^{(311)}s_{31})-\varphi_1sgn(\tilde{a}_1)|\tilde{a}_1|^\omega, & {}_0D_t^\alpha\{{}^{(122)}\hat{r}_{25}\}=m_1\lambda|{}^{(122)}s_{25}|,\\
{}_0D_t^\alpha\hat{b}_1=-\lambda a_{22}x_1({}^{(122)}s_{25})-\varphi_1sgn(\tilde{b}_1)|\tilde{b}_1|^\omega, & {}_0D_t^\alpha\{{}^{(244)}\hat{r}_{30}\}=m_1\lambda|{}^{(244)}s_{30}|,\\
{}_0D_t^\alpha\hat{c}_1=\lambda a_{33}x_3({}^{(433)}s_{36})-\varphi_1sgn(\tilde{c}_1)|\tilde{c}_1|^\omega, & {}_0D_t^\alpha\{{}^{(311)}\hat{r}_{31}\}=m_1\lambda|{}^{(311)}s_{31}|,\\
{}_0D_t^\alpha\hat{d}_1=-\lambda a_{44}x_4({}^{(244)}s_{30})-\varphi_1sgn(\tilde{d}_1)|\tilde{d}_1|^\omega, & {}_0D_t^\alpha\{{}^{(433)}\hat{r}_{36}\}=m_1\lambda|{}^{(433)}s_{36}|,\\
{}_0D_t^\alpha\hat{a}_2=-\lambda b_{11}(y_2-y_1)({}^{(311)}s_{31})\varphi_2sgn(\tilde{a}_2)|\tilde{a}_2|^\omega, & {}_0D_t^\alpha\{{}^{(122)}\hat{q}_{25}\}=m_2\lambda|{}^{(122)}s_{25}|,\\
{}_0D_t^\alpha\hat{b}_2=\lambda b_{33}y_3({}^{(433)}s_{36})-\varphi_2sgn(\tilde{b}_2)|\tilde{b}_2|^\omega, & {}_0D_t^\alpha\{{}^{(244)}\hat{q}_{30}\}=m_2\lambda|{}^{(244)}s_{30}|,\\
{}_0D_t^\alpha\hat{c}_2=-\lambda b_{22}y_2({}^{(122)}s_{25})-\varphi_2sgn(\tilde{c}_2)|\tilde{c}_2|^\omega, & {}_0D_t^\alpha\{{}^{(311)}\hat{q}_{31}\}=m_2\lambda|{}^{(311)}s_{31}|,\\
{}_0D_t^\alpha\hat{d}_2=-\lambda b_{22}y_1({}^{(122)}s_{25})-\varphi_2sgn(\tilde{d}_2)|\tilde{d}_2|^\omega, & {}_0D_t^\alpha\{{}^{(433)}\hat{q}_{36}\}=m_2\lambda|{}^{(433)}s_{36}|,\\
{}_0D_t^\alpha\hat{\mathrm{r}}=-\lambda b_{44}y_4({}^{(244)}s_{30})-\varphi_2sgn(\tilde{\mathrm{r}})|\tilde{\mathrm{r}}|^\omega, & \\
{}_0D_t^\alpha\hat{a}_3=\lambda c_{11}(z_2-z_1)({}^{(122)}s_{25})-\varphi_3sgn(\tilde{a}_3)|\tilde{a}_3|^\omega, & \\
{}_0D_t^\alpha\hat{b}_3=\lambda c_{22}z_2({}^{(244)}s_{30})-\varphi_3sgn(\tilde{b}_3)|\tilde{b}_3|^\omega, & \\
{}_0D_t^\alpha\hat{c}_3=-\lambda c_{33}z_3({}^{(311)}s_{31})-\varphi_3sgn(\tilde{c}_3)|\tilde{c}_3|^\omega, & \\
{}_0D_t^\alpha\hat{d}_3=\lambda c_{44}z_4({}^{(433)}s_{36})-\varphi_3sgn(\tilde{d}_3)|\tilde{d}_3|^\omega. &
\end{array}
$$

In this two numerical simulations, we adopt the matrices A,B,C as identity matrices. The initial values of the drive systems (31), (32) and response system (33) are selected as $x(0)=(2,-2,1,1)$, $y(0)=(1,1,2,2)$, $z(0)=(-20,3,1,3)$. The initial conditions of the unknown parameter in D-R system and upper bound of SD are selected as $(a_1(0),b_1(0),c_1(0),d_1(0))=(2,1,-2,1)$, $(a_2(0),b_2(0),c_2(0),d_2(0),\mathrm{r}(0))=(1,-3,1,1,-5)$, $(a_3(0),b_3(0),c_3(0),d_3(0))=(1,1,-2,-2)$, $(r_1(0),r_2(0),r_3(0),r_4(0))=(-2.5,1,-3,1)$, $(q_1(0),q_2(0),q_3(0),q_4(0))=(1,-2.5,-5,1)$. The constants $\lambda=2$, $m_1=10$, $m_2=10$, $k_1=10$, $\varphi_1=10$, $\varphi_2=10$, $\varphi_3=10$, $\omega=0.5$. For $\boldsymbol{e}=({}^{(124)}e_3,{}^{(243)}e_{12},{}^{(312)}e_{14},{}^{(431)}e_{24})^T$, the state trajectories about the error variables are drawn in Figure 2, the synchronization for the state trajectories of drive systems (31), (32) and response system (33) are drawn in Figure 3, the trajectories of estimations $\hat{\boldsymbol{\theta}}=(\hat{a}_1,\hat{b}_1,\hat{c}_1,\hat{d}_1)^T$, $\hat{\boldsymbol{\beta}}=(\hat{a}_2,\hat{b}_2,\hat{c}_2,\hat{d}_2,\hat{\mathrm{r}})^T$, $\hat{\boldsymbol{\vartheta}}=(\hat{a}_3,\hat{b}_3,\hat{c}_3,\hat{d}_3)^T$ are drawn in Figure 4, ${}^{(ijk)}\hat{r}_p$, and ${}^{(ijk)}\hat{q}_p$, $(p=1,2,3,4)$ are drawn in Figure 5. For $\boldsymbol{e}=({}^{(122)}e_{25},{}^{(244)}e_{30},{}^{(311)}e_{31},{}^{(433)}e_{36})^T$, the state trajectories about the error variables are drawn in Figure 6, the synchronization for the state trajectories of drive systems (31), (32) and response system (33) are drawn in Figure 7, the trajectories of estimations $\hat{\boldsymbol{\theta}}=(\hat{a}_1,\hat{b}_1,\hat{c}_1,\hat{d}_1)^T$, $\hat{\boldsymbol{\beta}}=(\hat{a}_2,\hat{b}_2,\hat{c}_2,\hat{d}_2,\hat{\mathrm{r}})^T$, $\hat{\boldsymbol{\vartheta}}=(\hat{a}_3,\hat{b}_3,\hat{c}_3,\hat{d}_3)^T$ are drawn in Figure 8, ${}^{(ijk)}\hat{r}_p$, and ${}^{(ijk)}\hat{q}_p$, $(p=1,2,3,4)$ are drawn in Figure 9. Motivated by the numerical simulation results, it can reveal that the drive systems (31), (32) and response system (33) achieve MSSMCS. Therefore, the multi-switching adaptive controllers (MSAC) (15) and some suitable multi-switching adaptive updating laws (MSAUL) (18) are effective.

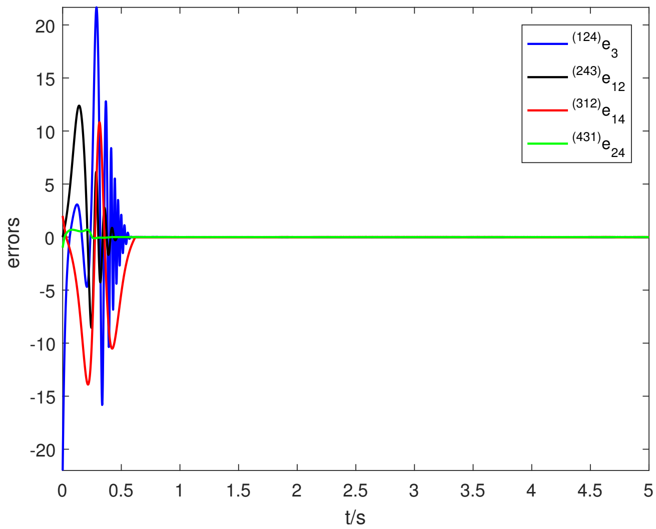

Figure 2. The synchronization errors $^{(124)}e_3,^{(243)}e_{12},^{(312)}e_{14},^{(431)}e_{24}$ change with time t.

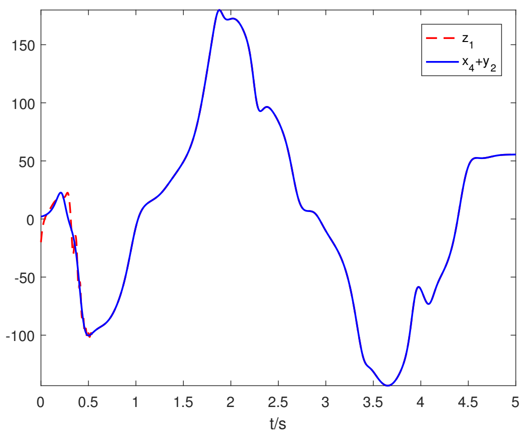

(**a**)

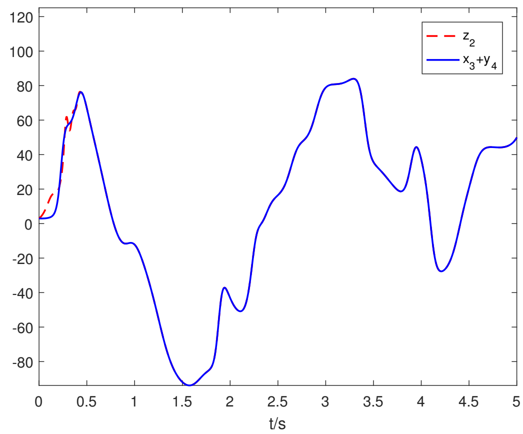

(**b**)

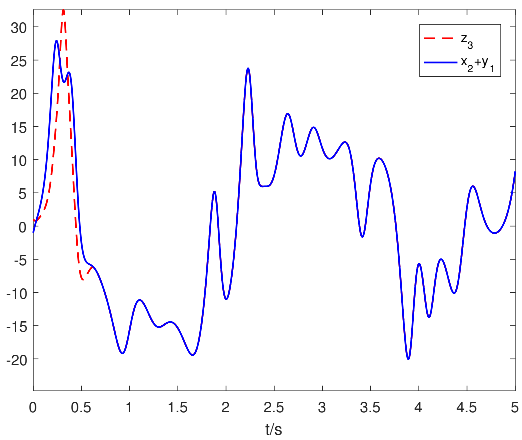

(**c**)

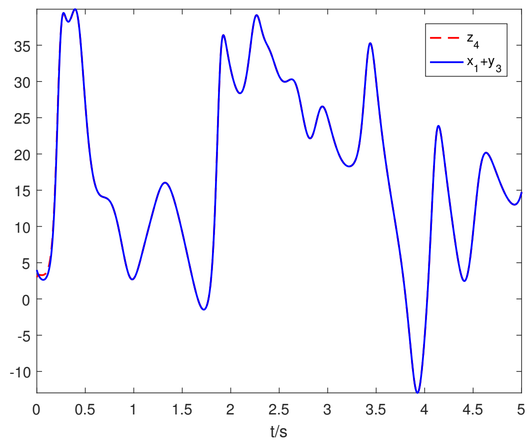

(**d**)

Figure 3. The synchronization for state variables z_1 and $x_4 + y_2$, z_2 and $x_3 + y_4$, z_3 and $x_2 + y_1$, z_4 and $x_1 + y_3$ of drive systems (31), (32) and response system (33) indicating in sub-pictures (**a**–**d**), respectively.

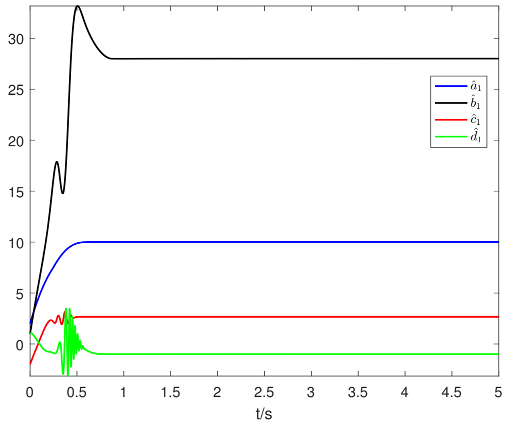

(**a**)

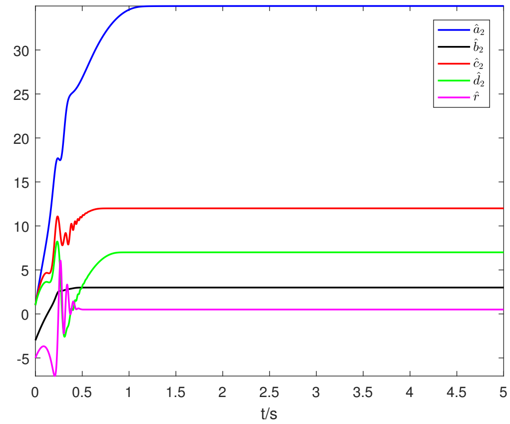

(**b**)

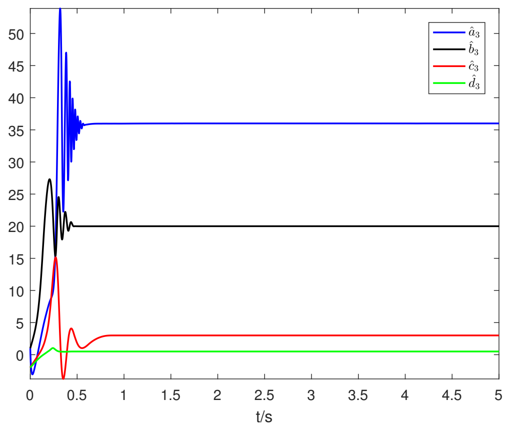

(**c**)

Figure 4. The estimation of parameters $\hat{a}_1, \hat{b}_1, \hat{c}_1, \hat{d}_1$ of drive system (31) (**a**), $\hat{a}_2, \hat{b}_2, \hat{c}_2, \hat{d}_2, \hat{r}$ of drive system (32) (**b**), $\hat{a}_3, \hat{b}_3, \hat{c}_3, \hat{d}_3$ of response system (33) (**c**).

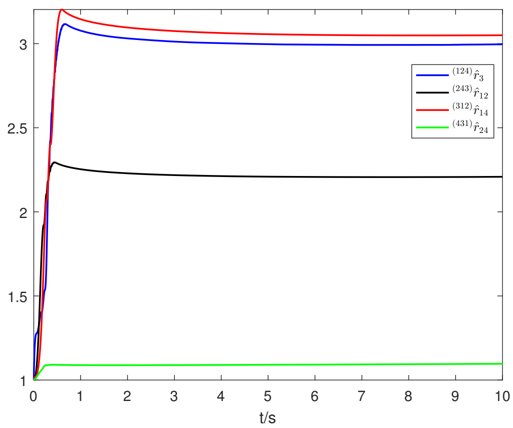

(**a**)

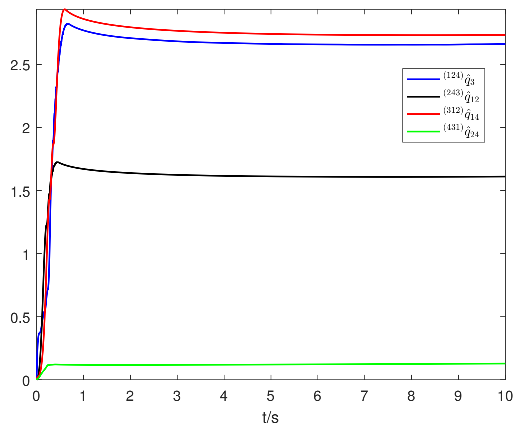

(**b**)

Figure 5. The estimation of parameters ${}^{(124)}\hat{r}_3$, ${}^{(243)}\hat{r}_{12}$, ${}^{(312)}\hat{r}_{14}$, ${}^{(431)}\hat{r}_{24}$ and ${}^{(124)}\hat{q}_3$, ${}^{(243)}\hat{q}_{12}$, ${}^{(312)}\hat{q}_{14}$, ${}^{(431)}\hat{q}_{24}$ shown in sub-pictures (**a**,**b**).

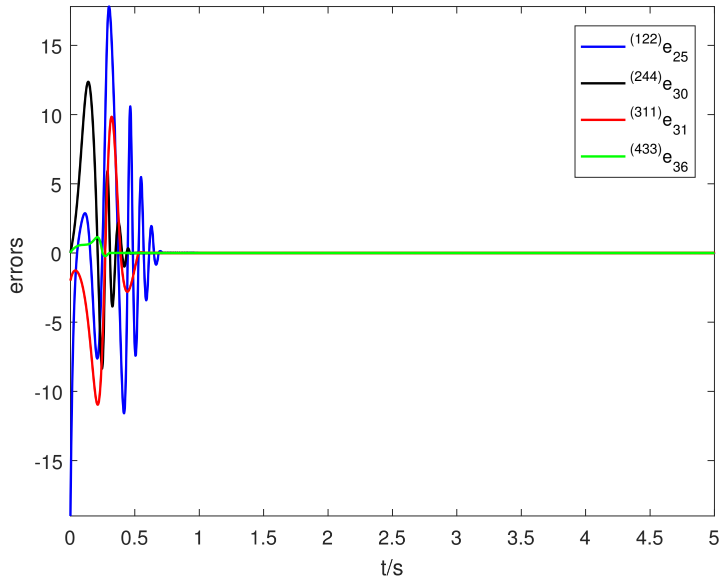

Figure 6. The synchronization errors $^{(122)}e_{25}, ^{(244)}e_{30}, ^{(311)}e_{31}, ^{(433)}e_{36}$ change with time t.

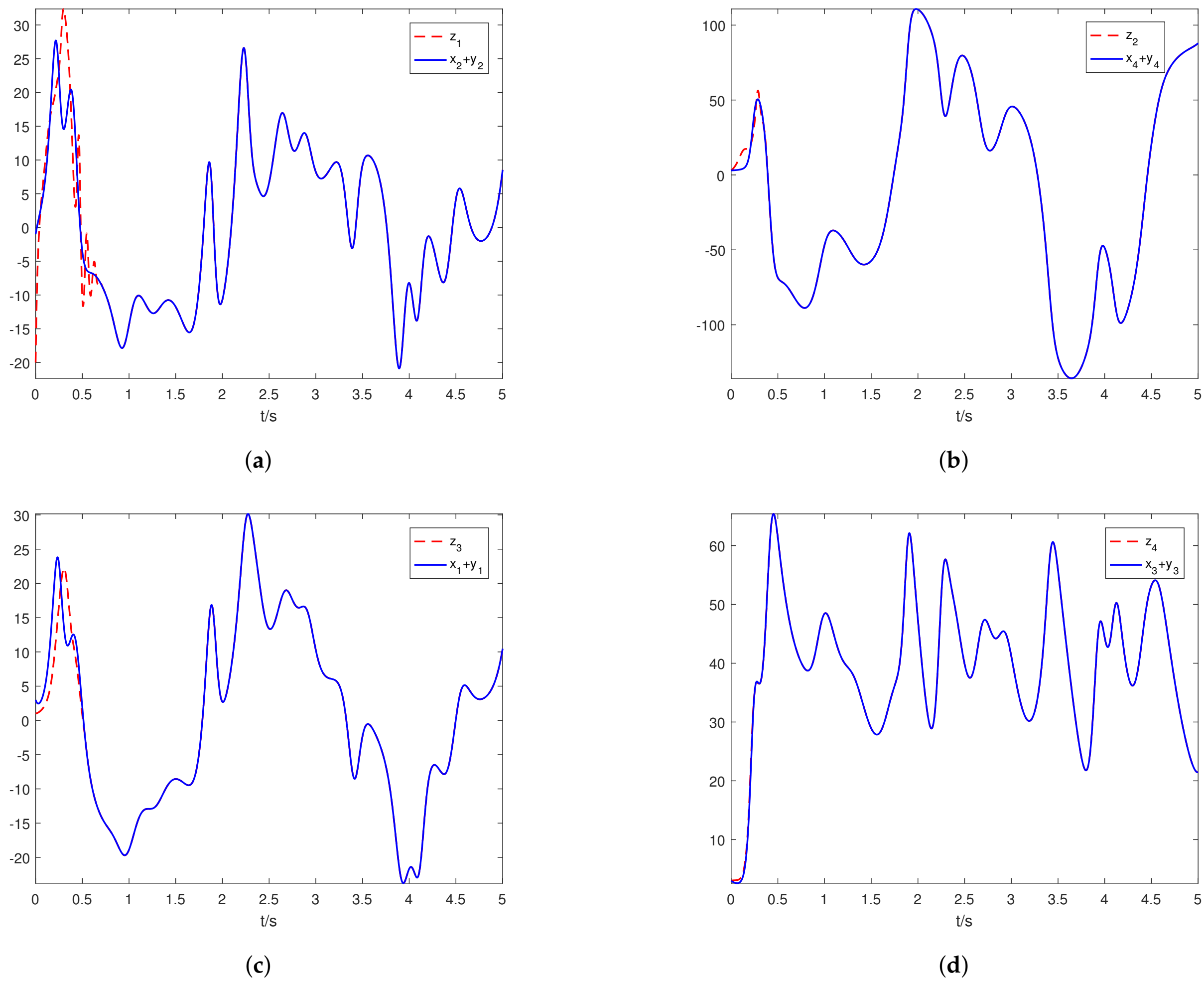

Figure 7. The synchronization for state variables z_1 and $x_2 + y_2$, z_2 and $x_4 + y_4$, z_3 and $x_1 + y_1$, z_4 and $x_3 + y_3$ of drive systems (31), (32) and response system (33) indicating in sub-pictures (**a**–**d**), respectively.

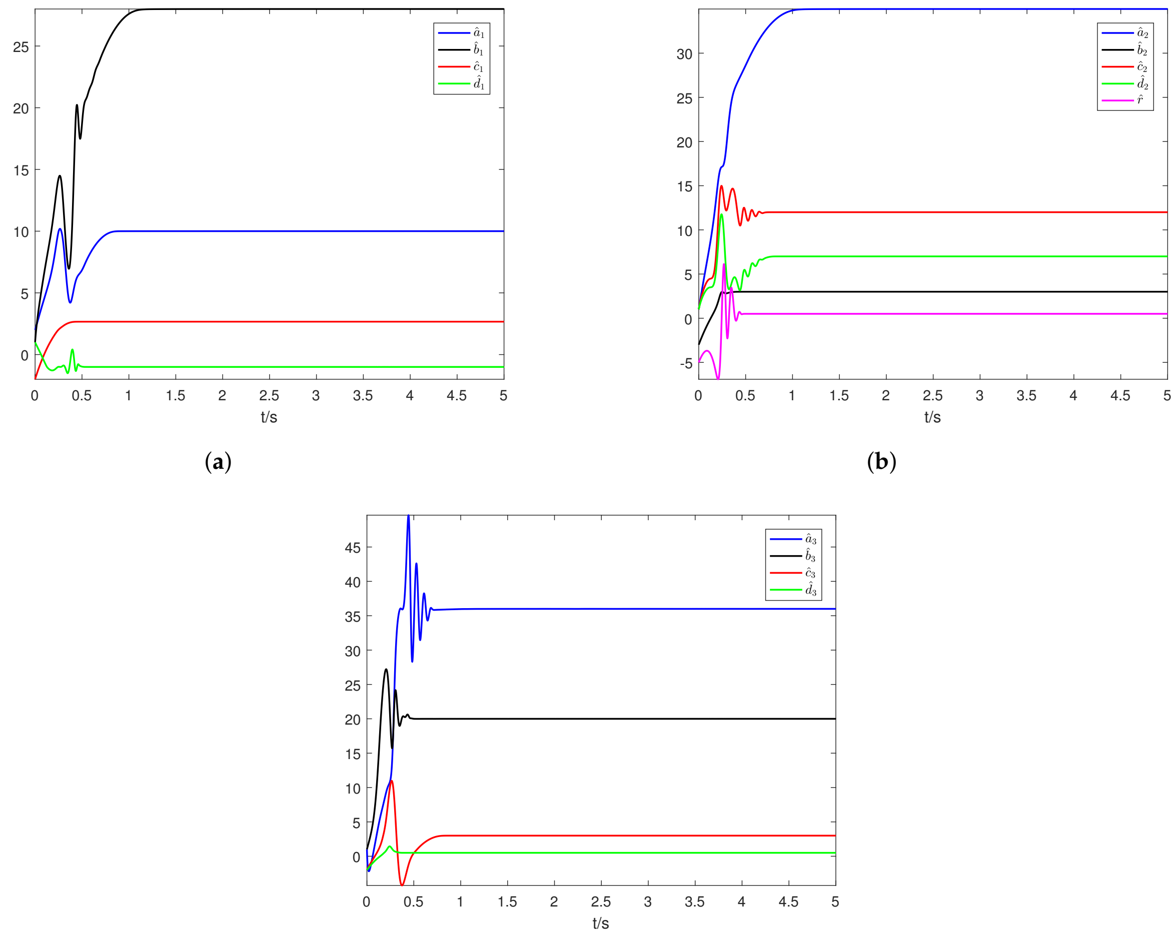

(**a**) (**b**)

(**c**)

Figure 8. The estimation of parameters $\hat{a}_1, \hat{b}_1, \hat{c}_1, \hat{d}_1$ of drive system (31) (**a**), $\hat{a}_2, \hat{b}_2, \hat{c}_2, \hat{d}_2, \hat{r}$ of drive system (32) (**b**), $\hat{a}_3, \hat{b}_3, \hat{c}_3, \hat{d}_3$ of response system (33) (**c**).

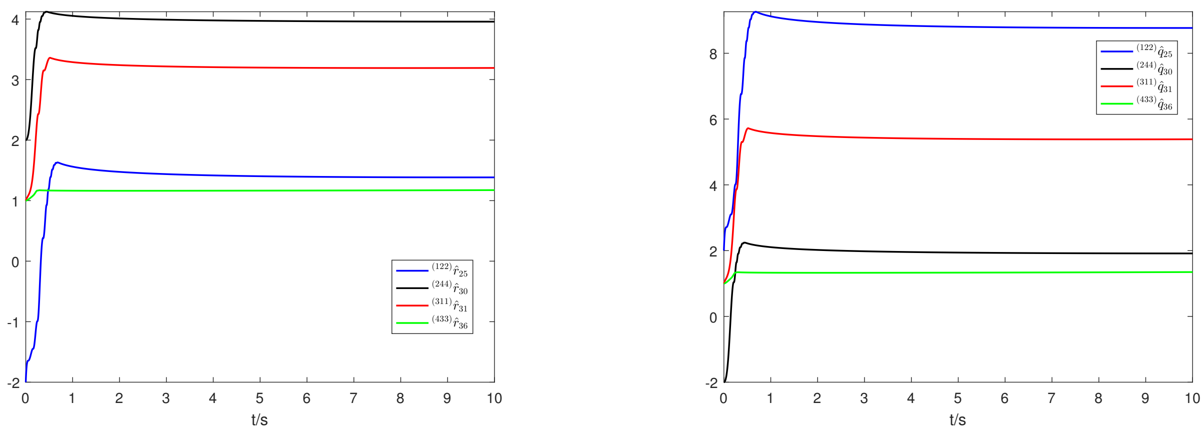

(**a**) (**b**)

Figure 9. The estimation of parameters ${}^{(122)}\hat{r}_{25}$, ${}^{(244)}\hat{r}_{30}$, ${}^{(311)}\hat{r}_{31}$, ${}^{(433)}\hat{r}_{36}$ and ${}^{(122)}\hat{q}_{25}$, ${}^{(244)}\hat{q}_{30}$, ${}^{(311)}\hat{q}_{31}$, ${}^{(433)}\hat{q}_{36}$ shown in sub-pictures (**a**,**b**).

6.2. Numerical Simulations for FO Chaotic System with Diffrenrt Dimensions

As an example, we choose FO Lorenz, Chen chaotic system as the drive systems, and the FO hyper-chaotic Lü system as the response system. Adding SD to the D-R systems, we obtain

$$\begin{pmatrix} {}_0D_t^{\alpha}x_1 \\ {}_0D_t^{\alpha}x_2 \\ {}_0D_t^{\alpha}x_3 \end{pmatrix} = \begin{pmatrix} x_2 - x_1 & 0 & 0 \\ 0 & x_1 & 0 \\ 0 & 0 & -x_3 \end{pmatrix} \begin{pmatrix} a_1 \\ b_1 \\ c_1 \end{pmatrix} + \begin{pmatrix} 0 + \Delta f_1 \\ -x_1x_3 - x_2 + \Delta f_2 \\ x_1x_2 + \Delta f_3 \end{pmatrix} + \begin{pmatrix} \mathrm{d}_1 \\ \mathrm{d}_2 \\ \mathrm{d}_3 \end{pmatrix}, \tag{43}$$

$$\begin{pmatrix} {}_0D_t^{\alpha}y_1 \\ {}_0D_t^{\alpha}y_2 \\ {}_0D_t^{\alpha}y_3 \end{pmatrix} = \begin{pmatrix} y_2 - y_1 & 0 & 0 \\ -y_1 & 0 & y_1 + y_2 \\ 0 & -y_3 & 0 \end{pmatrix} \begin{pmatrix} a_2 \\ b_2 \\ c_2 \end{pmatrix} + \begin{pmatrix} 0 + \Delta g_1 \\ -y_1y_3 + \Delta g_2 \\ y_1y_2 + \Delta g_3 \end{pmatrix} + \begin{pmatrix} D_1 \\ D_2 \\ D_3 \end{pmatrix}, \tag{44}$$

$$\begin{pmatrix} {}_0D_t^{\alpha}z_1 \\ {}_0D_t^{\alpha}z_2 \\ {}_0D_t^{\alpha}z_3 \\ {}_0D_t^{\alpha}z_4 \end{pmatrix} = \begin{pmatrix} z_2 - z_1 & 0 & 0 & 0 \\ 0 & z_2 & 0 & 0 \\ 0 & 0 & -z_3 & 0 \\ 0 & 0 & 0 & z_4 \end{pmatrix} \begin{pmatrix} a_3 \\ b_3 \\ c_3 \\ d_3 \end{pmatrix} + \begin{pmatrix} z_4 + \Delta h_1 \\ -z_1z_3 + \Delta h_2 \\ z_1z_2 + \Delta h_3 \\ z_1z_3 + \Delta h_4 \end{pmatrix} + \begin{pmatrix} \mu_1 + u_1 \\ \mu_2 + u_2 \\ \mu_3 + u_3 \\ \mu_4 + u_4 \end{pmatrix}, \tag{45}$$

Choosing the parameters are $a_1 = 10, b_1 = 28, c_1 = 8/3, a_2 = 35, b_2 = 3, c_2 = 28, a_3 = 36, b_3 = 20, c_3 = 3, d_3 = 0.5$. The initial conditions take as $x(0) = (2, -2, 1), y(0) = (1, -1, 3), z(0) = (-2, 3, 1, 3)$. When $\boldsymbol{\Delta g} = 0$, $\boldsymbol{\Delta f} = 0$, $\boldsymbol{\Delta h} = 0$, $\boldsymbol{d}(t) = 0$, $\boldsymbol{D}(t) = 0$, $\boldsymbol{\mu}(t) = 0$ and $\alpha = 0.97$, we can obtain the attractor graphs of the FO Lorenz and Chen chaotic system, which are presented in Figure 10. The attractor graphs of hyper-chaotic Lü system can be seen Figure 1.

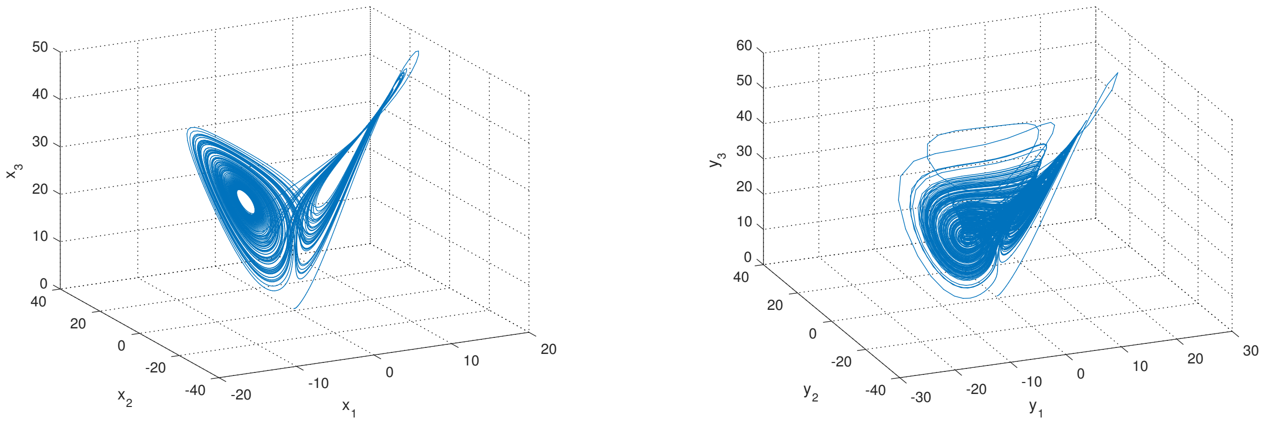

(a) **(b)**

Figure 10. The 3D phase plots of FO Lorenz chaotic system (**a**), FO Chen chaotic system (**b**).

Assume

$$A = B = \begin{pmatrix} 1 & 0 & 1 \\ 2 & 1 & 0 \\ 0 & 1 & 2 \\ 1 & 0 & 1 \end{pmatrix}, \quad C = \begin{pmatrix} 1 & 0 & 0 & 0 \\ 0 & 1 & 0 & 0 \\ 0 & 0 & 1 & 0 \\ 0 & 0 & 0 & 1 \end{pmatrix}. \tag{46}$$

In relation to (11), the multi-switching error state modes between the drive systems (43), (44) and the response system (45) are listed:

$$Switch\!-\!1 : l \neq w \neq v \begin{cases} {}^{(123)}e_1, & {}^{(132)}e_2, & {}^{(124)}e_3, & {}^{(142)}e_4, & {}^{(134)}e_5, & {}^{(143)}e_6, \\ {}^{(213)}e_7, & {}^{(231)}e_8, & {}^{(214)}e_9, & {}^{(241)}e_{10}, & {}^{(234)}e_{11}, & {}^{(243)}e_{12}, \\ {}^{(321)}e_{13}, & {}^{(312)}e_{14}, & {}^{(324)}e_{15}, & {}^{(314)}e_{16}, & {}^{(341)}e_{17}, & {}^{(342)}e_{18}, \\ {}^{(412)}e_{19}, & {}^{(421)}e_{20}, & {}^{(413)}e_{21}, & {}^{(423)}e_{22}, & {}^{(432)}e_{23}, & {}^{(431)}e_{24}. \end{cases}$$

$$Switch-2: l \neq w = v \begin{cases} {}^{(122)}e_{25}, & {}^{(133)}e_{26}, & {}^{(144)}e_{27}, & {}^{(211)}e_{28}, & {}^{(233)}e_{29}, & {}^{(244)}e_{30}, \\ {}^{(311)}e_{31}, & {}^{(322)}e_{32}, & {}^{(344)}e_{33}, & {}^{(411)}e_{34}, & {}^{(422)}e_{35}, & {}^{(433)}e_{36}. \end{cases}$$

$$Switch-3: l = w \neq v \begin{cases} {}^{(112)}e_{37}, & {}^{(113)}e_{38}, & {}^{(114)}e_{39}, & {}^{(221)}e_{40}, & {}^{(223)}e_{41}, & {}^{(224)}e_{42}, \\ {}^{(331)}e_{43}, & {}^{(332)}e_{44}, & {}^{(334)}e_{45}, & {}^{(441)}e_{46}, & {}^{(442)}e_{47}, & {}^{(443)}e_{48}. \end{cases}$$

$$Switch-4: l = v \neq w \begin{cases} {}^{(121)}e_{49}, & {}^{(131)}e_{50}, & {}^{(141)}e_{51}, & {}^{(212)}e_{52}, & {}^{(232)}e_{53}, & {}^{(242)}e_{54}, \\ {}^{(313)}e_{55}, & {}^{(323)}e_{56}, & {}^{(343)}e_{57}, & {}^{(414)}e_{58}, & {}^{(424)}e_{59}, & {}^{(434)}e_{60}. \end{cases}$$

$$Switch-5: l = w = v \begin{cases} {}^{(111)}e_{61}, & {}^{(222)}e_{62}, \\ {}^{(333)}e_{63}, & {}^{(444)}e_{64}. \end{cases}$$

In this section, we arbitrarily select the appropriate switching error variables for the situation of Switch-1 ($l \neq w \neq v$) from above, namely, $\boldsymbol{e} = ({}^{(142)}e_4, {}^{(234)}e_{12}, {}^{(321)}e_{13}, {}^{(413)}e_{21})^T$; For Switch-2 ($l \neq w = v$), we arbitrarily select $\boldsymbol{e} = ({}^{(122)}e_{25}, {}^{(244)}e_{30}, {}^{(311)}e_{31}, {}^{(433)}e_{36})^T$. Thus, the following two switching modes for numerical simulation are obtained:

$$Switch-1: \begin{cases} {}^{(142)}e_4 = [\sum_{i=1}^{4}(c_{1i}z_i) - \{\sum_{j=1}^{3}(b_{4j}y_j) + \sum_{k=1}^{3}(a_{2k}x_k)\}], \\ {}^{(234)}e_{12} = [\sum_{i=1}^{4}(c_{2i}z_i) - \{\sum_{j=1}^{3}(b_{3j}y_j) + \sum_{k=1}^{3}(a_{4k}x_k)\}], \\ {}^{(321)}e_{13} = [\sum_{i=1}^{4}(c_{3i}z_i) - \{\sum_{j=1}^{3}(b_{2j}y_j) + \sum_{k=1}^{3}(a_{1k}x_k)\}], \\ {}^{(413)}e_{21} = [\sum_{i=1}^{4}(c_{4i}z_i) - \{\sum_{j=1}^{3}(b_{1j}y_j) + \sum_{k=1}^{3}(a_{3k}x_k)\}], \end{cases} \tag{47}$$

$$Switch-2: \begin{cases} {}^{(122)}e_{25} = [\sum_{i=1}^{4}(c_{1i}z_i) - \{\sum_{j=1}^{3}(b_{2j}y_j) + \sum_{k=1}^{3}(a_{2k}x_k)\}], \\ {}^{(244)}e_{30} = [\sum_{i=1}^{4}(c_{2i}z_i) - \{\sum_{j=1}^{3}(b_{4j}y_j) + \sum_{k=1}^{3}(a_{4k}x_k)\}], \\ {}^{(311)}e_{31} = [\sum_{i=1}^{4}(c_{3i}z_i) - \{\sum_{j=1}^{3}(b_{1j}y_j) + \sum_{k=1}^{3}(a_{1k}x_k)\}], \\ {}^{(433)}e_{36} = [\sum_{i=1}^{4}(c_{4i}z_i) - \{\sum_{j=1}^{3}(b_{3j}y_j) + \sum_{k=1}^{3}(a_{3k}x_k)\}], \end{cases} \tag{48}$$

In order to exhibit the effectiveness of the designed MSAC (25) and the MSAUL (28), the nonlinear uncertainties and external disturbances are assumed as follows:

$$\begin{aligned} \boldsymbol{d}(\boldsymbol{x}(t)) &= (-0.1cos(t), -0.2cos(2t), 0.3sin(3t))^T, \\ \boldsymbol{D}(\boldsymbol{y}(t)) &= (-0.1sin(t), -0.2sin(2t), 0.3cos(3t))^T, \\ \boldsymbol{\mu}(\boldsymbol{z}(t)) &= (0.1cos(5t), 0.2cos(6t), 0.3sin(7t), 0.4sin(8t))^T, \\ \Delta\boldsymbol{f}(\boldsymbol{x}(t)) &= (0.1cos(2tx_1), 0.2cos(2tx_2), 0.3sin(2tx_3))^T, \\ \Delta\boldsymbol{g}(\boldsymbol{y}(t)) &= (0.1sin(2\pi t), 0.2sin(sgn(y_2)), 0.3cos(2\pi y_3))^T, \\ \Delta\boldsymbol{h}(\boldsymbol{z}(t)) &= (0.1sin(2tsgn(z_1)), 0.2sin(2tsgn(z_2)), 0.3sin(3t), 0.4sin(4t))^T. \end{aligned}$$

6.2.1. Switch-1

It follows from Switch-1 (47) that the FO error dynamic systems are expressed as:

$$
\begin{aligned}
{}_0D_t^{\alpha}\{{}^{(142)}e_4\} =& [\sum_{i=1}^{4} c_{1i}({}_0D_t^{\alpha}z_i) - \{\sum_{j=1}^{3} b_{4j}({}_0D_t^{\alpha}y_j) + \sum_{k=1}^{3} a_{2k}({}_0D_t^{\alpha}x_k)\}] \\
=& \{(z_2 - z_1)a_3 + z_4 + \Delta h_1 + \mu_1 + {}^{(142)}u_4\} \\
& -\{(y_2 - y_1)a_2 - y_3 b_2 + y_1 y_2 + \Delta g_1 + \Delta g_3 + D_1 + D_3\} \\
& -\{2(x_2 - x_1)a_1 + x_1 b_1 - x_1 x_3 - x_2 + 2\Delta f_1 + \Delta f_2 + 2\mathrm{d}_1 + \mathrm{d}_2\}, \\
{}_0D_t^{\alpha}\{{}^{(234)}e_{12}\} =& [\sum_{i=1}^{4} c_{2i}({}_0D_t^{\alpha}z_i) - \{\sum_{j=1}^{3} b_{3j}({}_0D_t^{\alpha}y_j) + \sum_{k=1}^{3} a_{4k}({}_0D_t^{\alpha}x_k)\}] \\
=& \{z_2 b_3 - z_1 z_3 + \Delta h_2 + \mu_2 + {}^{(234)}u_{12}\} - \{-y_1 a_2 - 2y_3 b_2 \\
& +(y_2 + y_1)c_2 - y_1 y_3 + 2y_1 y_2 + \Delta g_2 + 2\Delta g_3 + D_2 + 2D_3\} \\
& -\{(x_2 - x_1)a_1 - x_3 c_1 + x_1 x_2 + \Delta f_1 + \Delta f_3 + \mathrm{d}_1 + \mathrm{d}_3\}, \\
{}_0D_t^{\alpha}\{{}^{(321)}e_{13}\} =& [\sum_{i=1}^{4} c_{3i}({}_0D_t^{\alpha}z_i) - \{\sum_{j=1}^{3} b_{2j}({}_0D_t^{\alpha}y_j) + \sum_{k=1}^{3} a_{1k}({}_0D_t^{\alpha}x_k)\}] \\
=& \{-z_3 c_3 + z_1 z_2 + \Delta h_3 + \mu_3 + {}^{(321)}u_{13}\} - \{2(y_2 - 2y_1)a_2 \\
& +(y_1 + y_2)c_2 - y_1 a_2 - y_1 y_3 + 2\Delta g_1 + \Delta g_2 + 2D_1 + D_2\} \\
& -\{(x_2 - x_1)a_1 - x_3 c_1 - x_1 x_2 + \Delta f_1 + \Delta f_3 + \mathrm{d}_1 + \mathrm{d}_3\}, \\
{}_0D_t^{\alpha}\{{}^{(413)}e_{21}\} =& [\sum_{i=1}^{4} c_{4i}({}_0D_t^{\alpha}z_i) - \{\sum_{j=1}^{3} b_{1j}({}_0D_t^{\alpha}y_j) + \sum_{k=1}^{3} a_{3k}({}_0D_t^{\alpha}x_k)\}] \\
=& \{z_4 d_3 + z_1 z_3 + \Delta h_4 + \mu_4 + {}^{(413)}u_{21}\} \\
& -\{(y_2 - y_1)a_2 - y_3 b_2 + y_1 y_2 + \Delta g_1 + \Delta g_3 + D_1 + D_3\} \\
& -\{x_1 b_1 - 2x_3 c_1 - x_1 x_3 - x_2 + 2x_1 x_2 + \Delta f_2 + 2\Delta f_3 + \mathrm{d}_2 + 2\mathrm{d}_3\}.
\end{aligned}
$$

It follows from the forms of MSAC (25) and MSAUL (28) that the controllers are designed as follows:

$$
\begin{aligned}
{}^{(142)}u_4 =& -z_4 + y_1 y_2 - x_1 x_3 - x_2 - \hat{a}_3(z_2 - z_1) + \hat{a}_2(y_2 - y_1) - \hat{b}_1 y_3 \\
& +2\hat{a}_1(x_2 - x_1) + \hat{b}_1 x_1 - ({}^{(142)}\hat{\rho}_4 + {}^{(142)}\hat{\varrho}_4)sgn({}^{(142)}s_4) - k_1 sgn({}^{(142)}s_4), \\
{}^{(234)}u_{12} =& z_1 z_3 - y_1 y_3 + 2y_1 y_2 + x_1 x_2 - \hat{b}_3 z_2 - \hat{a}_2 y_1 - 2\hat{b}_2 y_3 + \hat{c}_2(y_1 + y_2) \\
& +\hat{a}_1(x_2 - x_1) - \hat{c}_1 x_3 - ({}^{(234)}\hat{\rho}_{12} + {}^{(234)}\hat{\varrho}_{12})sgn({}^{(234)}s_{12}) - k_1 sgn({}^{(234)}s_{12}), \\
{}^{(321)}u_{13} =& -z_1 z_2 - y_1 y_3 + x_1 x_2 + \hat{c}_3 z_3 - \hat{a}_2 y_3 + 2\hat{a}_2(y_2 - 2y_1) + \hat{c}_2(y_1 + y_2) \\
& +\hat{a}_1(x_2 - x_1) - \hat{c}_1 x_3 - ({}^{(321)}\hat{\rho}_{13} + {}^{(321)}\hat{\varrho}_{13})sgn({}^{(321)}s_{13}) - k_1 sgn({}^{(321)}s_{13}), \\
{}^{(413)}u_{21} =& -z_1 z_3 + y_1 y_2 - x_1 x_3 - x_2 + 2x_1 x_2 - \hat{d}_3 z_4 + \hat{a}_2(y_2 - y_1) - \hat{b}_2 y_3 \\
& +\hat{b}_1 x_1 - 2\hat{c}_1 x_3 - ({}^{(413)}\hat{\rho}_{21} + {}^{(413)}\hat{\varrho}_{21})sgn({}^{(413)}s_{21}) - k_1 sgn({}^{(413)}s_{21}),
\end{aligned}
$$

and the parameters updating laws are designed as follows:

$$
\begin{aligned}
{}_0D_t^{\alpha}\hat{b}_1 &= -\lambda x_1\{({}^{(142)}s_4) + ({}^{(413)}s_{21})\} - \varphi_1 sgn(\tilde{b}_1)(|\tilde{b}_1|^{\omega}), \\
{}_0D_t^{\alpha}\hat{c}_1 &= \lambda x_3\{({}^{(234)}s_{12}) + ({}^{(321)}s_{13}) + 2({}^{(142)}s_4)\} - \varphi_1 sgn(\tilde{c}_1)(|\tilde{c}_1|^{\omega}), \\
{}_0D_t^{\alpha}\hat{b}_2 &= \lambda y_3\{({}^{(142)}s_4) + 2({}^{(234)}s_{12}) + ({}^{(413)}s_{21})\} - \varphi_2 sgn(\tilde{b}_2)(|\tilde{b}_2|^{\omega}), \\
{}_0D_t^{\alpha}\hat{c}_2 &= -\lambda(y_1 + y_2)\{({}^{(234)}s_{12}) + ({}^{(321)}s_{13})\} - \varphi_2 sgn(\tilde{c}_2)(|\tilde{c}_2|^{\omega}), \\
{}_0D_t^{\alpha}\hat{a}_3 &= \lambda(z_2 - z_1)({}^{(142)}s_4) - \varphi_3 sgn(\tilde{a}_3)(|\tilde{a}_3|^{\omega}),
\end{aligned}
$$

$$
\begin{aligned}
&{}_0D_t^\alpha \hat{b}_3 = \lambda z_2({}^{(234)}s_{12}) - \varphi_3 sgn(\tilde{b}_3)(|\tilde{b}_3|^\omega),\\
&{}_0D_t^\alpha \hat{c}_3 = -\lambda z_3({}^{(321)}s_{13}) - \varphi_3 sgn(\tilde{c}_3)(|\tilde{c}_3|^\omega),\\
&{}_0D_t^\alpha \hat{d}_3 = \lambda z_4({}^{(413)}s_{21}) - \varphi_3 sgn(\tilde{d}_3)(|\tilde{d}_3|^\omega),\\
&{}_0D_t^\alpha \hat{a}_1 = -\lambda(x_2 - x_1)\{({}^{(321)}s_{13}) + ({}^{(234)}s_{12}) + 2({}^{(413)}s_{21})\} - \varphi_1 sgn(\tilde{a}_1)(|\tilde{a}_1|^\omega),\\
&{}_0D_t^\alpha \hat{a}_2 = -\lambda\{(y_2 - y_1)(({}^{(142)}s_4) + ({}^{(413)}s_{21}) + 2({}^{(321)}s_{13})) - y_3(({}^{(234)}s_{12}) + ({}^{(321)}s_{13}))\}\\
&\qquad - \varphi_1 sgn(\tilde{a}_2)(|\tilde{a}_2|^\omega),
\end{aligned}
$$

$$
\begin{aligned}
&{}_0D_t^\alpha\{{}^{(142)}\hat{\rho}_4\} = m_1\lambda|{}^{(142)}s_4|, && {}_0D_t^\alpha\{{}^{(234)}\hat{\rho}_{12}\} = m_1\lambda|{}^{(234)}s_{12}|,\\
&{}_0D_t^\alpha\{{}^{(321)}\hat{\rho}_{13}\} = m_1\lambda|{}^{(321)}s_{13}|, && {}_0D_t^\alpha\{{}^{(413)}\hat{\rho}_{21}\} = m_1\lambda|{}^{(413)}s_{21}|,\\
&{}_0D_t^\alpha\{{}^{(142)}\hat{\varrho}_4\} = m_2\lambda|{}^{(142)}s_4|, && {}_0D_t^\alpha\{{}^{(234)}\hat{\varrho}_{12}\} = m_2\lambda|{}^{(234)}s_{12}|,\\
&{}_0D_t^\alpha\{{}^{(321)}\hat{\varrho}_{13}\} = m_2\lambda|{}^{(321)}s_{13}|, && {}_0D_t^\alpha\{{}^{(413)}\hat{\varrho}_{21}\} = m_2\lambda|{}^{(413)}s_{21}|.
\end{aligned}
$$

6.2.2. Switch-2

It follows from Switch-2 (48) that the FO error dynamic systems are expressed as:

$$
\begin{aligned}
{}_0D_t^\alpha\{{}^{(122)}e_{25}\} =& [\sum_{i=1}^{4} c_{1i}({}_0D_t^\alpha z_i) - \{\sum_{j=1}^{3} b_{2j}({}_0D_t^\alpha y_j) + \sum_{k=1}^{3} a_{2k}({}_0D_t^\alpha x_k)\}]\\
=& \{(z_2 - z_1)a_3 + z_4 + \Delta h_1 + \mu_1 + {}^{(122)}u_{25}\} - \{2(y_2 - y_1)a_2\\
& - y_1a_2 + (y_1 + y_2)c_2 - y_1y_3 + 2\Delta g_1 + \Delta g_2 + 2D_1 + D_2\}\\
& - \{2(x_2 - x_1)a_1 + x_1b_1 - x_1x_3 - x_2 + 2\Delta f_1 + \Delta f_2 + 2\mathrm{d}_1 + \mathrm{d}_2\},\\
{}_0D_t^\alpha\{{}^{(244)}e_{30}\} =& [\sum_{i=1}^{4} c_{2i}({}_0D_t^\alpha z_i) - \{\sum_{j=1}^{3} b_{4j}({}_0D_t^\alpha y_j) + \sum_{k=1}^{3} a_{4k}({}_0D_t^\alpha x_k)\}]\\
=& \{z_2b_3 - z_1z_3 + \Delta h_2 + \mu_2 + {}^{(244)}u_{30}\}\\
& - \{(y_2 - y_1)a_2 - y_3b_2 + y_1y_2 + \Delta g_1 + \Delta g_3 + D_1 + D_3\}\\
& - \{(x_2 - x_1)a_1 - x_3c_1 + x_1x_2 + \Delta f_1 + \Delta f_3 + \mathrm{d}_1 + \mathrm{d}_3\},\\
{}_0D_t^\alpha\{{}^{(311)}e_{31}\} =& [\sum_{i=1}^{4} c_{3i}({}_0D_t^\alpha z_i) - \{\sum_{j=1}^{3} b_{1j}({}_0D_t^\alpha y_j) + \sum_{k=1}^{3} a_{1k}({}_0D_t^\alpha x_k)\}]\\
=& \{-z_3c_3 + z_1z_2 + \Delta h_3 + \mu_3 + {}^{(311)}u_{31}\}\\
& - \{(y_2 - y_1)a_2 - y_3b_2 + y_1y_2 + \Delta g_1 + \Delta g_3 + D_1 + D_3\}\\
& - \{(x_2 - x_1)a_1 - x_3c_1 + x_1x_2 + \Delta f_1 + \Delta f_3 + \mathrm{d}_1 + \mathrm{d}_3\},\\
{}_0D_t^\alpha\{{}^{(433)}e_{36}\} =& [\sum_{i=1}^{4} c_{4i}({}_0D_t^\alpha z_i) - \{\sum_{j=1}^{3} b_{3j}({}_0D_t^\alpha y_j) + \sum_{k=1}^{3} a_{3k}({}_0D_t^\alpha x_k)\}]\\
=& \{z_4d_3 + z_1z_3 + \Delta h_4 + \mu_4 + {}^{(433)}u_{36}\} - \{-y_1a_2 - 2y_3b_2\\
& + (y_2 + y_1)c_2 - y_1y_3 + 2y_1y_2 + \Delta g_2 + 2\Delta g_3 + D_2 + 2D_3\}\\
& - \{x_1b_1 - 2x_3c_1 - x_1x_3 - x_2 + 2x_1x_2 + \Delta f_2 + 2\Delta f_3 + \mathrm{d}_2 + 2\mathrm{d}_3\}.
\end{aligned}
$$

It follows from the forms of MSAC (25) and MSAUL (28) that the controllers are designed as follows:

$$
\begin{aligned}
{}^{(122)}u_{25} =& - z_4 - y_1y_3 - x_1x_3 - x_2 - \hat{a}_3(z_2 - z_1) + 2\hat{a}_2(y_2 - 2y_1) + \hat{c}_2(y_1 + y_2) - \hat{a}_2y_1\\
& + 2\hat{a}_1(x_2 - x_1) + \hat{b}_1x_1 - ({}^{(122)}\hat{\rho}_{25} + {}^{(122)}\hat{\varrho}_{25})sgn({}^{(122)}s_{25}) - k_1 sgn({}^{(122)}s_{25}),\\
{}^{(244)}u_{30} =& z_1z_3 + y_1y_2 + x_1x_2 - \hat{b}_3z_2 + \hat{a}_2(y_2 - y_1) - \hat{b}_1y_3\\
& + \hat{a}_1(x_2 - x_1) - \hat{c}_1x_3 - ({}^{(244)}\hat{\rho}_{30} + {}^{(244)}\hat{\varrho}_{30})sgn({}^{(244)}s_{30}) - k_1 sgn({}^{(244)}s_{30}),\\
{}^{(311)}u_{31} =& - z_1z_2 + y_1y_2 + x_1x_2 + \hat{c}_3z_3 + \hat{a}_2(y_2 - y_1) - \hat{b}_2y_3
\end{aligned}
$$

$$+\hat{a}_1(x_2-x_1)-\hat{c}_1x_3-({}^{(311)}\hat{\rho}_{31}+{}^{(311)}\hat{\varrho}_{31})sgn({}^{(311)}s_{31})-k_1sgn({}^{(311)}s_{31}),$$
$$\begin{aligned}{}^{(433)}u_{36}=&-z_1z_3-y_1y_3+2y_1y_2-x_1x_3-x_2+2x_1x_2-\hat{d}_3z_4-\hat{a}_2y_1-2\hat{b}_2y_3+\hat{c}_2(y_1+y_2)\\&+\hat{b}_1x_1-2\hat{c}_1x_3-({}^{(433)}\hat{\rho}_{36}+{}^{(433)}\hat{\varrho}_{36})sgn({}^{(433)}s_{36})-k_1sgn({}^{(433)}s_{36}).\end{aligned}$$

and the parameters updating laws are designed as follows:

$$\begin{aligned}{}_0D_t^{\alpha}\{{}^{(122)}\hat{\rho}_{25}\}&=m_1\lambda|{}^{(122)}s_{25}|, & {}_0D_t^{\alpha}\{{}^{(244)}\hat{\rho}_{30}\}&=m_1\lambda|{}^{(244)}s_{30}|,\\ {}_0D_t^{\alpha}\{{}^{(311)}\hat{\rho}_{31}\}&=m_1\lambda|{}^{(311)}s_{31}|, & {}_0D_t^{\alpha}\{{}^{(433)}\hat{\rho}_{36}\}&=m_1\lambda|{}^{(433)}s_{36}|,\\ {}_0D_t^{\alpha}\{{}^{(122)}\hat{\varrho}_{25}\}&=m_2\lambda|{}^{(122)}s_{25}|, & {}_0D_t^{\alpha}\{{}^{(244)}\hat{\varrho}_{30}\}&=m_2\lambda|{}^{(244)}s_{30}|,\\ {}_0D_t^{\alpha}\{{}^{(311)}\hat{\varrho}_{31}\}&=m_2\lambda|{}^{(311)}s_{31}|, & {}_0D_t^{\alpha}\{{}^{(433)}\hat{\varrho}_{36}\}&=m_2\lambda|{}^{(433)}s_{36}|,\end{aligned}$$

$$\begin{aligned}{}_0D_t^{\alpha}\hat{a}_1&=-\lambda(x_2-x_1)\{{}^{(311)}s_{31}+{}^{(244)}s_{30}+2({}^{(433)}s_{36})\}-\varphi_1sgn(\tilde{a}_1)(|\tilde{a}_1|^{\omega}),\\ {}_0D_t^{\alpha}\hat{b}_1&=-\lambda x_1\{{}^{(122)}s_{25}+{}^{(433)}s_{36}\}-\varphi_1sgn(\tilde{b}_1)(|\tilde{b}_1|^{\omega}),\\ {}_0D_t^{\alpha}\hat{c}_1&=\lambda x_3\{{}^{(244)}s_{30}+{}^{(311)}s_{31}+2({}^{(122)}s_{25})\}-\varphi_1sgn(\tilde{c}_1)(|\tilde{c}_1|^{\omega}),\\ {}_0D_t^{\alpha}\hat{a}_2&=-\lambda((y_2-y_1)\{{}^{(244)}s_{30}+2({}^{(433)}s_{36})+{}^{(311)}s_{31}\}-y_1\{{}^{(122)}s_{25}+{}^{(433)}s_{36}\})\\&\quad-\varphi_2sgn(\tilde{a}_2)(|\tilde{a}_2|^{\omega}),\\ {}_0D_t^{\alpha}\hat{b}_2&=\lambda y_3\{{}^{(244)}s_{30}+2({}^{(122)}s_{25})+{}^{(311)}s_{31}\}-\varphi_2sgn(\tilde{b}_2)(|\tilde{b}_2|^{\omega}),\\ {}_0D_t^{\alpha}\hat{c}_2&=-\lambda(y_1+y_2)({}^{(122)}s_{25}+{}^{(433)}s_{36})-\varphi_2sgn(\tilde{c}_2)(|\tilde{c}_2|^{\omega}),\\ {}_0D_t^{\alpha}\hat{a}_3&=\lambda(z_2-z_1)({}^{(122)}s_{25})-\varphi_3sgn(\tilde{a}_3)(|\tilde{a}_3|^{\omega}),\\ {}_0D_t^{\alpha}\hat{b}_3&=\lambda z_2({}^{(244)}s_{30})-\varphi_3sgn(\tilde{b}_3)(|\tilde{b}_3|^{\omega}),\\ {}_0D_t^{\alpha}\hat{c}_3&=-\lambda z_3({}^{(311)}s_{31})-\varphi_3sgn(\tilde{c}_3)(|\tilde{c}_3|^{\omega}),\\ {}_0D_t^{\alpha}\hat{d}_3&=\lambda z_4({}^{(433)}s_{36})-\varphi_3sgn(\tilde{d}_3)(|\tilde{d}_3|^{\omega}).\end{aligned} \tag{49}$$

In these two numerical simulations, the definition of matrices A, B, C are shown in (46). The initial conditions of the drive systems (43), (44) and response system (45) are selected as $x(0)=(2,-2,1)$, $y(0)=(1,1,2)$, $z(0)=(-20,3,1,3)$. The initial values of the unknown parameter in D-R system and upper bound of SD are, respectively, selected as $(a_1(0),b_1(0),c_1(0))=(2,1,-2)$, $(a_2(0),b_2(0),c_2(0))=(1,-3,1)$, $(a_3(0),b_3(0),c_3(0),d_3(0)) =(1,1,-2,-2)$, $(\rho_1(0),\rho_2(0),\rho_3(0),\rho_4(0))=(-2.5,1,-3,1)$, $(\varrho_1(0),\varrho_2(0),\varrho_3(0),\varrho_4(0))= (1,-2.5,-5,1)$. The constants $\lambda=2$, $m_1=10$, $m_2=10$, $k_1=10$, $\varphi_1=10$, $\varphi_2=10$, $\varphi_3=10$, $\omega=0.5$. For $\boldsymbol{e}=({}^{(142)}e_4,{}^{(234)}e_{12},{}^{(321)}e_{13},{}^{(413)}e_{21})^T$, the state trajectories about the error variables are drawn in Figure 11, the synchronization for the state trajectories of drive systems (43), (44) and response system (45) are drawn in Figure 12, the trajectories of estimations $\hat{\boldsymbol{\theta}}=(\hat{a}_1,\hat{b}_1,\hat{c}_1)^T$, $\hat{\boldsymbol{\beta}}=(\hat{a}_2,\hat{b}_2,\hat{c}_2)^T$, $\hat{\boldsymbol{\vartheta}}=(\hat{a}_3,\hat{b}_3,\hat{c}_3,\hat{d}_3)^T$ are drawn in Figure 13, ${}^{(lwv)}\hat{\rho}_p$, and ${}^{(lwv)}\hat{\varrho}_p$ are drawn in Figures 14. For $\boldsymbol{e}=({}^{(122)}e_{25},{}^{(244)}e_{30},{}^{(311)}e_{31},{}^{(433)}e_{36})^T$, the state trajectories about the error variables are drawn in Figure 15, the synchronization for the state trajectories of drive systems (43), (44) and response system (45) are drawn in Figure 16, the trajectories of estimations $\hat{\boldsymbol{\theta}}=(\hat{a}_1,\hat{b}_1,\hat{c}_1)^T$, $\hat{\boldsymbol{\beta}}=(\hat{a}_2,\hat{b}_2,\hat{c}_2)^T$, $\hat{\boldsymbol{\vartheta}}=(\hat{a}_3,\hat{b}_3,\hat{c}_3,\hat{d}_3)^T$ are drawn in Figures 17, ${}^{(lwv)}\hat{\rho}_p$, and ${}^{(lwv)}\hat{\varrho}_p$ are drawn in Figure 18. Motivated by the numerical simulation results, it can reveal that the drive systems (43), (44) and response system (45) achieve MSSMCS. Therefore, the multi-switching adaptive controllers (MSAC) (25) and some suitable multi-switching adaptive updating laws (MSAUL) (28) are effective.

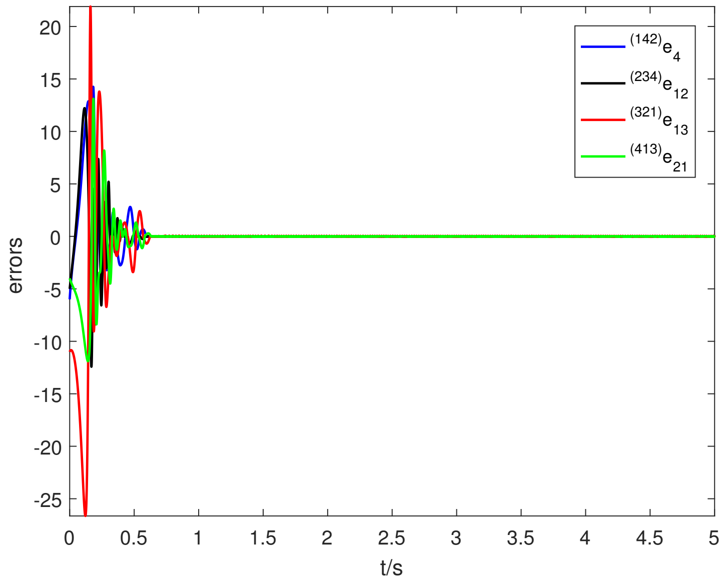

Figure 11. The synchronization errors $^{(142)}e_4$, $^{(234)}e_{12}$, $^{(321)}e_{13}$, $^{(413)}e_{21}$ change with time t.

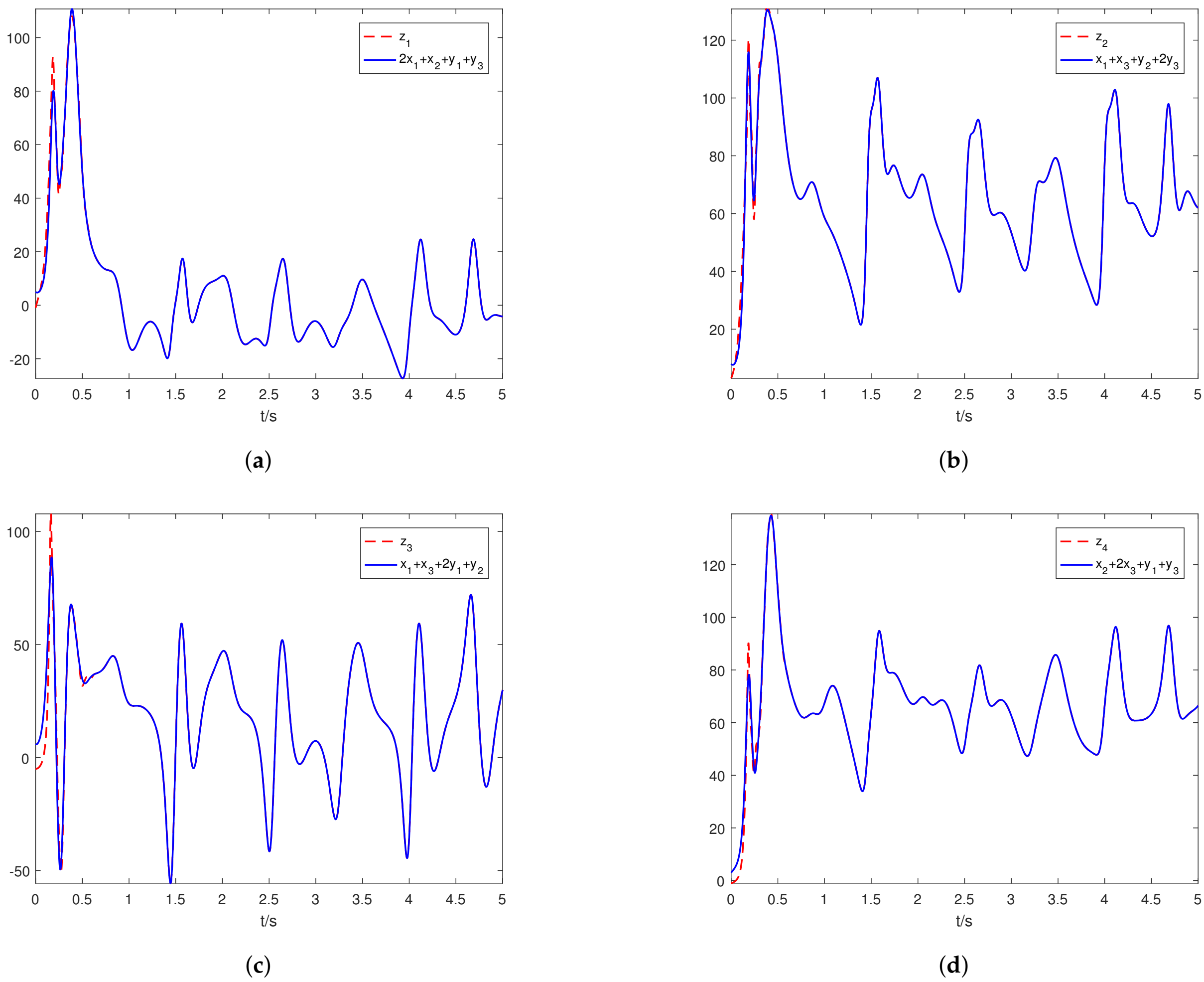

Figure 12. The synchronization for state variables z_1 and $2x_1 + x_2 + y_1 + y_3$, z_2 and $x_1 + x_3 + y_2 + 2y_3$, z_3 and $x_1 + x_3 + 2y_1 + y_2$, z_4 and $x_2 + 2x_3 + y_1 + y_3$ of drive systems (43), (44) and response system (45) indicating in sub-pictures (**a–d**), respectively.

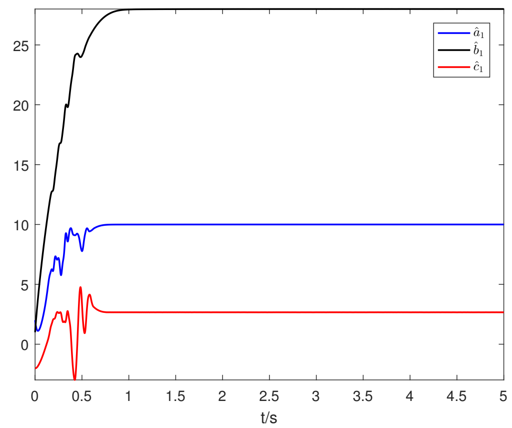

(**a**)

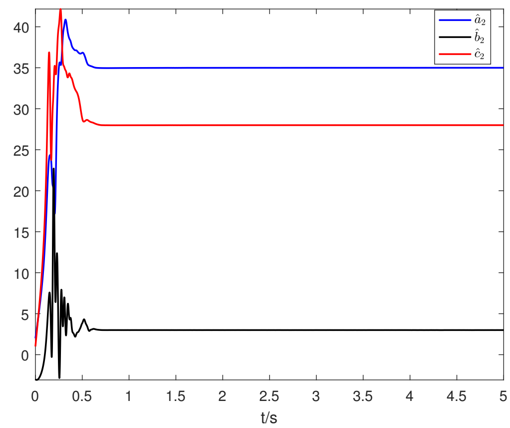

(**b**)

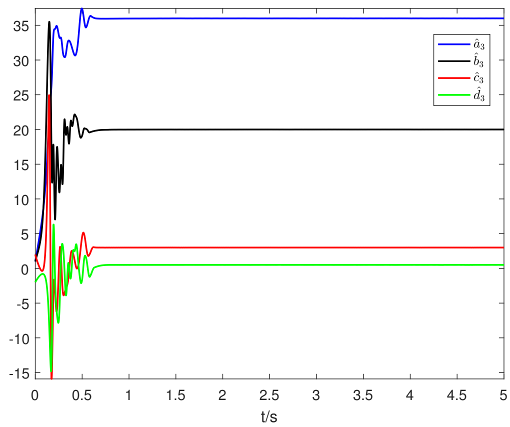

(**c**)

Figure 13. The estimation of parameters $\hat{a}_1, \hat{b}_1, \hat{c}_1$ of drive system (43) (**a**), $\hat{a}_2, \hat{b}_2, \hat{c}_2$ of drive system (44) (**b**), $\hat{a}_3, \hat{b}_3, \hat{c}_3, \hat{d}_3$ of drive system (45) (**c**).

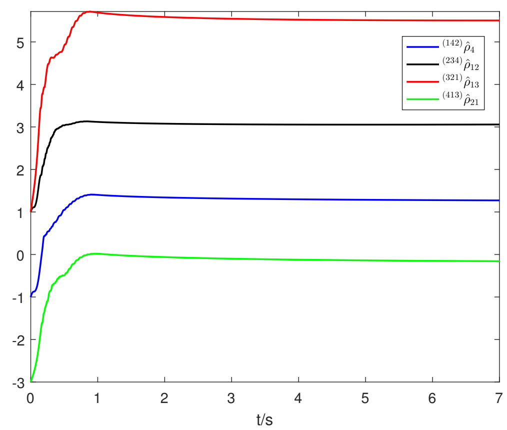

(**a**)

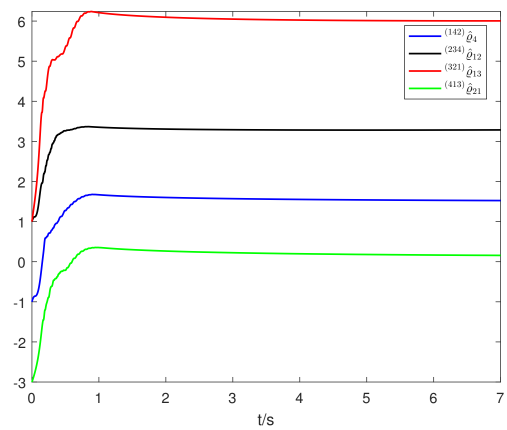

(**b**)

Figure 14. The estimation of parameters ${}^{(142)}\hat{\rho}_4$, ${}^{(234)}\hat{\rho}_{12}$, ${}^{(321)}\hat{\rho}_{13}$, ${}^{(413)}\hat{\rho}_{21}$ and ${}^{(142)}\hat{\varrho}_4$, ${}^{(234)}\hat{\varrho}_{12}$, ${}^{(321)}\hat{\varrho}_{13}$, ${}^{(413)}\hat{\varrho}_{21}$ shown in sub-pictures (**a**,**b**).

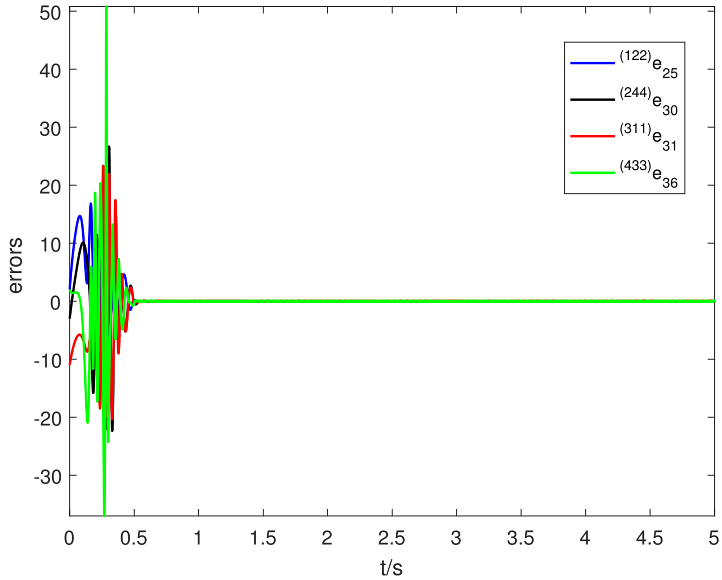

Figure 15. The synchronization errors ${}^{(122)}e_{25}$, ${}^{(244)}e_{30}$, ${}^{(311)}e_{31}$, ${}^{(433)}e_{36}$ change with time t.

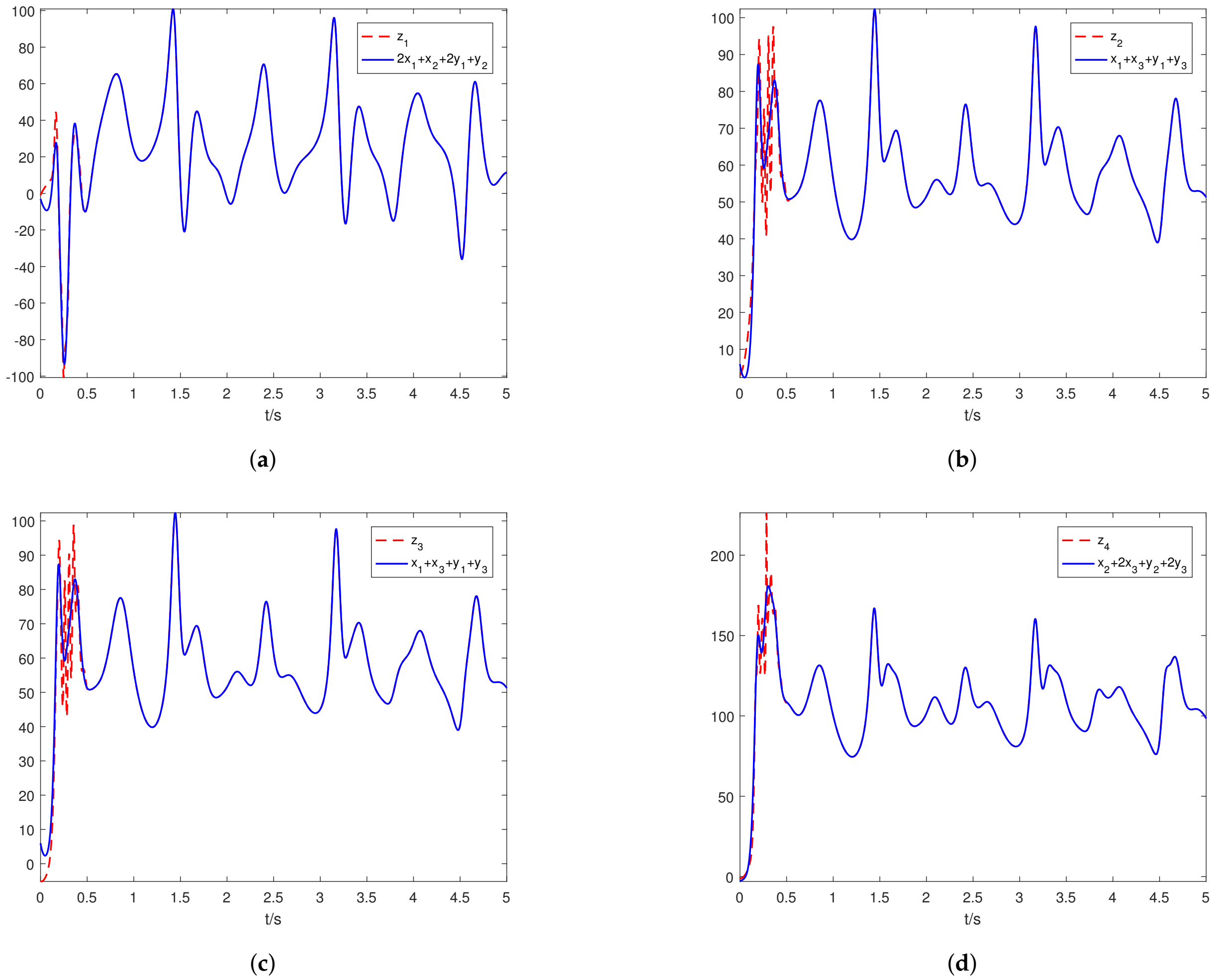

Figure 16. The synchronization for state variables z_1 and $2x_1 + x_2 + 2y_1 + y_2$, z_2 and $x_1 + x_3 + y_1 + y_3$, z_3 and $x_1 + x_3 + y_1 + y_3$, z_4 and $x_2 + 2x_3 + y_2 + 2y_3$ of drive systems (43), (44) and response system (45) indicating in sub-pictures (**a**–**d**), respectively.

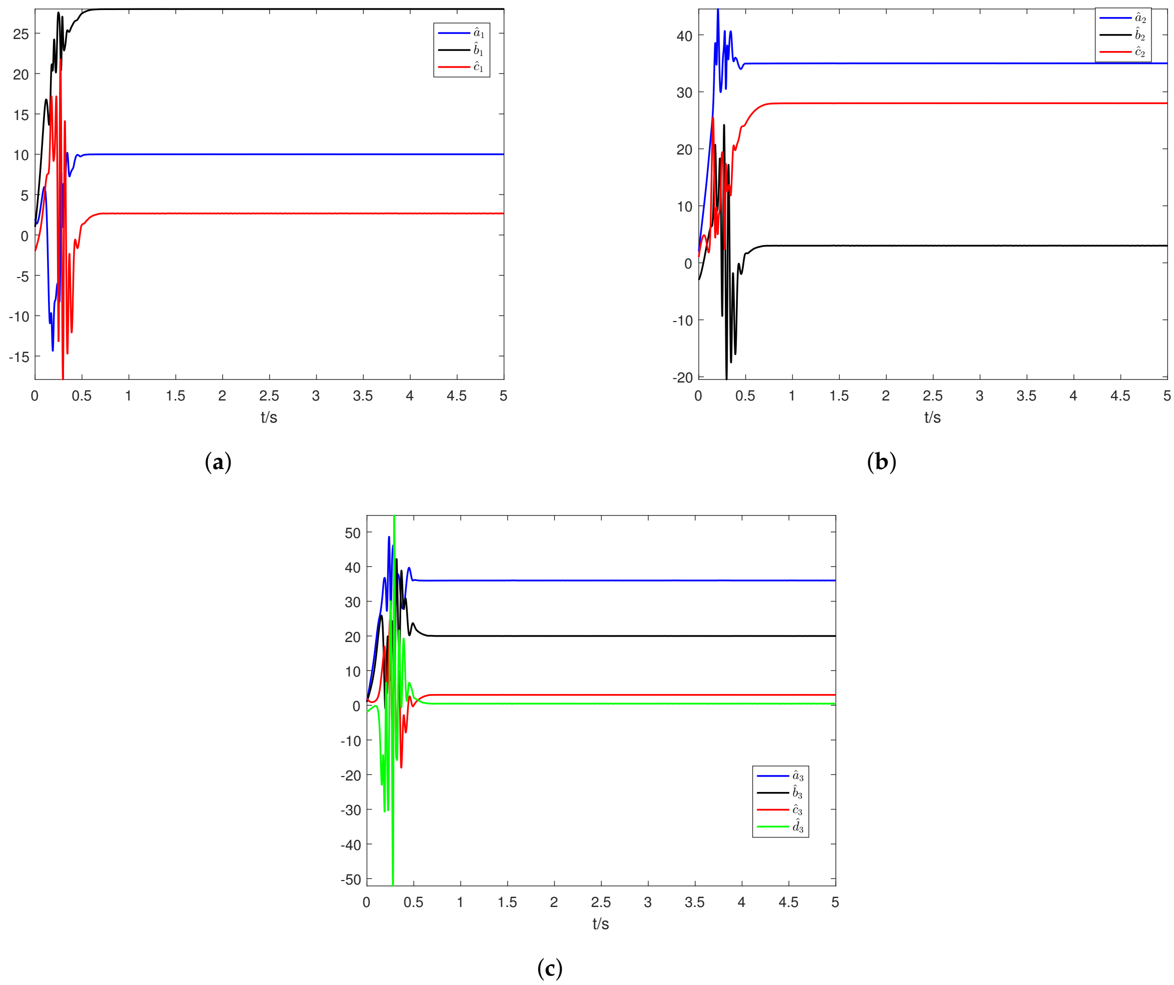

Figure 17. The estimation of parameters $\hat{a}_1, \hat{b}_1, \hat{c}_1$ of drive system (43) (**a**), $\hat{a}_2, \hat{b}_2, \hat{c}_2$ of drive system (44) (**b**), $\hat{a}_3, \hat{b}_3, \hat{c}_3, \hat{d}_3$ of drive system (46) (**c**).

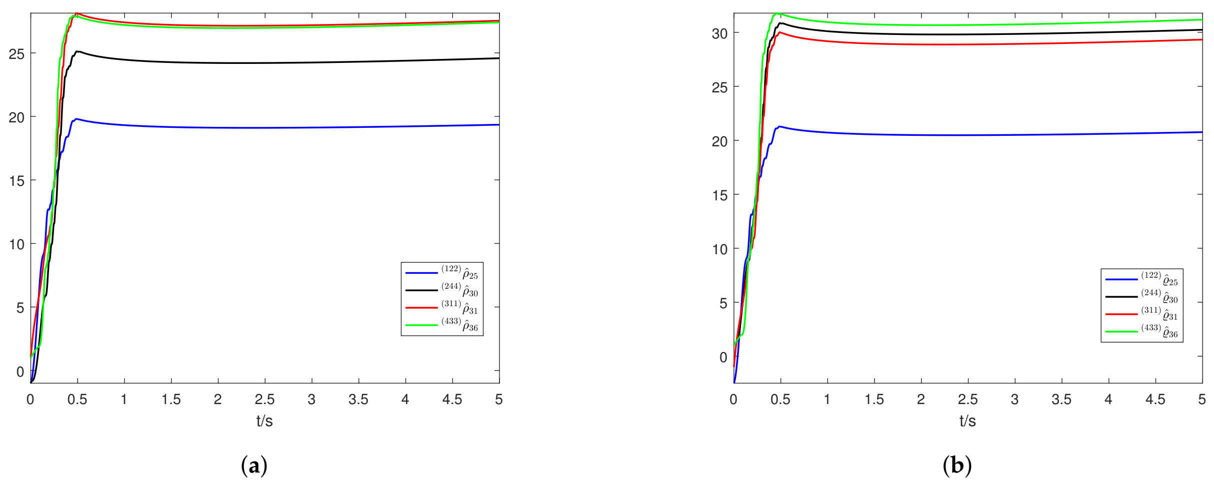

Figure 18. The estimation of parameters ${}^{(122)}\hat{\rho}_{25}$, ${}^{(244)}\hat{\rho}_{30}$, ${}^{(311)}\hat{\rho}_{31}$, ${}^{(433)}\hat{\rho}_{36}$ and ${}^{(122)}\hat{\varrho}_{25}$, ${}^{(244)}\hat{\varrho}_{30}$, ${}^{(311)}\hat{\varrho}_{31}$, ${}^{(433)}\hat{\varrho}_{36}$ shown in sub-pictures (**a**,**b**).

7. Conclusions

In this article, we investigated the multi-switching sliding mode combination synchronization (MSSMCS) of fractional order (FO) non-identical chaotic systems with unknown parameters and double stochastic disturbances (SD). In the theoretical parts, the FO chaotic systems with the different (or same) dimensions are considered. Our idea for this topic is that with the help of the Lyapunov theory and sliding mode control technique, we put forward a fractional order sliding surface, multi-switching adaptive controllers (MSAC) and multi-switching adaptive updating laws (MSAUL) that can achieve the state variables of the drive systems are synchronized with the different state variables of the response systems. Meanwhile, the unknown parameters are identified and upper bound values of stochastic disturbances are examined accurately. What's more, the combination drive systems and single response system we chose are very general. The different description of the scale matrices can make the multi-switching projection synchronization, multi-switching complete synchronization, multi-switching anti-synchronization, etc., become the special cases of MSSMCS. Motivated by the numerical simulation results, it is clear that the different error variables quickly converge to the equilibrium point. Therefore, the multi-switching adaptive controllers (MSAC) are effective and robust. Next, we will concentrate on the fractional order multi-switching synchronization of time-delay systems under multiple stochastic disturbances, and the parameters of system are still unknown.

Author Contributions: W.P. proposed the main the idea and Y.W. prepared the manuscript initially. T.L. gave the numerical simulation of this paper. All authors have read and agreed to the published version of the manuscript.

Funding: This work is partly supported by the Project of the Science and Technology Department in Sichuan Province (Grant No.2019YJ0456, 2021ZYD0004), Fund of Sichuan University of Science and Engineering (Grant No. 2020RC26, 2020RC42).

Institutional Review Board Statement: Not applicable.

Informed Consent Statement: Not applicable.

Data Availability Statement: The data used to support the findings of this study are available from the corresponding author upon request.

Acknowledgments: The authors would like to thank the editor and the anonymous reviewers for their constructive comments and suggestions to improve the quality of the paper.

Conflicts of Interest: The authors declare that they have no competing interests.

References

1. Ping, Z.; Peng, Z. Drive-response synchronization for chaotic systems. *J. Chongqing Univ.* **2002**, *25*, 77–79.
2. Yu, J.; Hu, C.; Jiang, H. Projective synchronization for fractional neural networks. *Neural Netw.* **2014**, *49*, 87–95. [CrossRef] [PubMed]
3. Shao, K.; Guo, H.; Han, F. Finite-time projective synchronization of fractional-order chaotic systems via soft variable structure control. *J. Mech. Sci. Technol.* **2020**, *34*, 369–376. [CrossRef]
4. Qin, X.; Li, S.; Liu, H. Adaptive fuzzy synchronization of uncertain fractional-order chaotic systems with different structures and time-delays. *Adv. Diff. Equ.* **2019**, *2019*, 1–16. [CrossRef]
5. Bouzeriba, A.; Boulkroune, A.; Bouden, T. Fuzzy adaptive synchronization of a class of fractional-order chaotic systems. *Int. J. Mach. Learn. Cybern.* **2016**, *7*, 1–16. [CrossRef]
6. Liu, Y.J.; Gong, M.; Tong, S.; Chen, C.P.; Li, D.J. Adaptive fuzzy output feedback control for a class of nonlinear systems with full state constraints. *IEEE Trans. Fuzzy. Syst.* **2018**, *26*, 2607–2617. [CrossRef]
7. Ha, S.; Chen, L.; Liu, H. Command filtered adaptive neural network synchronization control of fractional-order chaotic systems subject to unknown dead zones. *J. Frankl. Inst.* **2021**, *358*, 3376–3402. [CrossRef]
8. Zeng, H.B.; Teo, K.L.; He, Y.; Xu, H.; Wang, W. Sampled-data synchronization control for chaotic neural networks subject to actuator saturation. *Neurocomputing* **2017**, *185*, 1656–1667. [CrossRef]
9. Wang, J.; Xu, C. Stochastic feedback coupling synchronization of networked harmonic oscillators. *Automatica* **2018**, *87*, 404–411. [CrossRef]
10. Li, H.L.; Jiang, Y.L.; Wang, Z.; Zhang, L.; Teng, Z. Parameter identification and adaptive-impulsive synchronization of uncertain complex networks with nonidentical topological structures. *Optik-Int. J. Light Electron Opt.* **2015**, *126*, 5771–5776. [CrossRef]
11. Li, X.F.; Chu, Y.D.; Leung, A.Y.; Zhang, H. Synchronization of uncertain chaotic systems via complete-adaptive-impulsive controls. *Chaos Solitons Fractals* **2017**, *100*, 24–30. [CrossRef]
12. Kocamaz, U.E.; Cevher, B.; Uyaroğlu, Y. Control and synchronization of chaos with sliding mode control based on cubic reaching rule. *Chaos Solitons Fractals* **2017**, *105*, 92–98. [CrossRef]

13. Vaidyanathan, S. Anti-synchronization of 3-cells cellular neural network attractors via integral sliding mode control. *Int. J. PharmTech Res.* **2016**, *9*, 193–205.
14. Li, X.; Zhao, X.S. The chaotic synchronization of fractional-order and integer-order in a class of financial systems. *J. Sci. Teach. Coll. Univ.* **2020**, *40*, 1–4.
15. Jing, W.; Guang, P. Desgn of a sliding mode controller for synchronization of fractional-order chaotic systems with different structures. *J. Shanghai Jiaotong Univ.* **2016**, *50*, 849–853. 860.
16. Jiang, N. The adaptive control synchronization of hyper-chaos lorenz system and hyper-chaos Rössler system. *J. Taiyuan Norm Univ.* **2014**, *13*, 47–50.
17. Wei, X. Adaptive control and synchronization of Lü hyper-chaotic system. *J. Honghe Univ.* **2015**, *13*, 23–27.
18. Li, T.; Wang, Y.; Zhao, C. Synchronization of fractional chaotic systems based on a simple Lyapunov function. *Adv. Diff. Equ.* **2017**, *2017*, 304. [CrossRef]
19. Wei, Y.H.; Chen, Y.Q. Lyapunov functions for nabla discrete fractional order systems. *ISA Trans.* **2019**, *88*, 82–90. [CrossRef]
20. Khan, A.; Jahanzaib, L.S. Synchronization on the adaptive sliding mode controller for fractional order complex chaotic systems with uncertainty and disturbances. *Int. J. Dyn. Control.* **2019**, *7*, 1419–1433. [CrossRef]
21. Luo, R.; Su, H.; Zeng, Y. Synchronization of uncertain fractional-order chaotic systems via a novel adaptive controller. *Chin. J. Phys.* **2017**, *55*, 342–349. [CrossRef]
22. Zhang, R.; Yang, S. Robust chaos synchronization of fractional-order chaotic systems with unknown parameters and uncertain perturbations. *Nonlinear Dyn.* **2012**, *69*, 983–992. [CrossRef]
23. Ma, S.J.; Shen, Q.; Jing, H. Modified projective synchronization of stochastic fractional order chaotic systems with uncertain parameters. *Nonlinear Dyn.* **2013**, *73*, 93–100. [CrossRef]
24. Wang, Q.; Qi, D.L. Synchronization for fractional order chaotic systems with uncertain parameters. *Int. J. Control. Autom. Syst.* **2016**, *14*, 211–216. [CrossRef]
25. Nian, F.; Liu, X.; Zhang, Y. Sliding mode synchronization of fractional-order complex chaotic system with parametric and external disturbances. *Chaos Solitons Fractals* **2018**, *116*, 22–28. [CrossRef]
26. Zhang, X.; Zhang, X.; Li, D.; Yang, D. Adaptive synchronization for a class of fractional order time-delay uncertain chaotic systems via fuzzy fractional order neural network. *Int. J. Control. Autom. Syst.* **2019**, *17*, 1209–1220. [CrossRef]
27. Deepika, D.; Kaur, S.; Narayan, S. Uncertainty and disturbance estimator based robust synchronization for a class of uncertain fractional chaotic system via fractional order sliding mode control. *Chao Solitons Fractals* **2018**, *115*, 196–203. [CrossRef]
28. Luo, R.; Wang, Y.L.; Deng, S.C. Combination synchronization of three classic chaotic systems using active backstepping desgn. *Chaos* **2011**, *21*, 043114.
29. Khan, A.; Nigar, U. Adaptive hybrid complex projective combination-combination synchronization in non-identical hyper-chaotic complex systems. *Int. J. Dynam. Control.* **2019**, *7*, 1404–1418. [CrossRef]
30. Vincent, U.E.; Saseyi, A.O.; Mcclintock, P. Multi-switching combination synchronization of chaotic systems. *Nonlinear Dyn.* **2015**, *80*, 845–854. [CrossRef]
31. Sun, J.; Cui, G.; Wang, Y.; Shen, Y. Combination complex synchronization of three chaotic complex systems. *Nonlinear Dyn.* **2015**, *79*, 953–965. [CrossRef]
32. Khan, ; A.; Budhraja, M.; Ibraheem, A. Combination-combination synchronisation of time-delay chaotic systems for unknown parameters with uncertainties and external disturbances. *Pramana* **2018**, *91*, 20. [CrossRef]
33. Sun, J.; Wang, Y.; Wang, Y.; Cui, G.; Shen, Y. Compound-combination synchronization of five chaotic systems via nonlinear control. *Optik-Int. J. Light Electron. Opt.* **2016**, *127*, 4136–4143. [CrossRef]
34. Khan, A.; Trikha, P. Compound difference anti-synchronization between chaotic systems of integer and fractional order. *SN Appl. Sci.* **2019**, *1*, 1–13. [CrossRef]
35. Yadav, V.K.; Prasad, G.; Srivastava, M.; Das, S. Triple compound synchronization among eight chaotic systems with external disturbances via nonlinear approach. *Differ. Equ. Dyn. Syst.* **2019**, *2019*, 1–24. [CrossRef]
36. Zhang, B.; Deng, F. Double-compound synchronization of six memristor-based Lorenz systems. *Nonlinear Dyn.* **2014**, *77*, 1519–1530. [CrossRef]
37. Mahmoud, G.M.; Abed-Elhameed, T.M.; Farghaly, A.A. Double compound combination synchronization among eight n-dimensional chaotic systems. *Chin. Phys. B* **2018**, *27*, 154–162. [CrossRef]
38. Khan, A.; Khattar, D.; Prajapati, N. Dual combination combination multi switching synchronization of eight chaotic systems. *Chin. J. Phys.* **2017**, *55*, 1209–1218. [CrossRef]
39. Ahmad, I.; Shafiq, M.; Al-Sawalha, M.M. Globally exponential multi switching-combination synchronization control of chaotic systems for secure communications. *Chin. J. Phys.* **2018**, *56*, 974–987. [CrossRef]
40. Zheng, S. Multi-switching combination synchronization of three different chaotic systems via nonlinear control. *Optik-Int. J. Light Electron. Opt.* **2016**, *127*, 10247–10258. [CrossRef]
41. Khan, A.; Budhraja, M.; Ibraheem, A. Synchronization among different switches of four non-identical chaotic systems via adaptive control. *Arabian J. Sci. Eng.* **2019**, *44*, 2717–2728. [CrossRef]
42. Aysha, I. Multi-switching dual combination synchronization of time delay dynamical systems for fully unknown parameters via adaptive control. *Arabian J. Sci. Eng.* **2020**, *45*, 6911–6922.

43. Shafiq, M.; Ahmad, I. Multi-Switching combination anti-synchronization of unknown hyper-chaotic systems. *Arabian J. Sci. Eng.* **2019**, *44*, 1–16. [CrossRef]
44. Song, S.; Song, X.N.; Pathak, N.; Balsera, I.T. Multi-switching adaptive synchronization of two fractional-order chaotic systems with different structure and different order. *Int. J. Control. Autom. Syst.* **2017**, *15*, 1524–1535. [CrossRef]
45. Shahzad, M. Multi-switching synchronization of different orders: A generalization of increased/reduced order synchronization. *Iran. J. Sci. Technol.* **2020**, *44*, 167–176. [CrossRef]
46. Chen, X.; Park, J.H.; Cao, J.; Qiu, J. Adaptive synchronization of multiple uncertain coupled chaotic systems via sliding mode control. *Neurocomputing* **2018**, *273*, 9–21. [CrossRef]
47. Chen, X.; Cao, J.; Park, J.H.; Huang, T.; Qiu, J. Finite-time multi-switching synchronization behavior for multiple chaotic systems with network transmission mode. *J. Frankl. Inst.* **2018**, *355*, 2892–2911. [CrossRef]
48. Modiri, A.; Mobayen, S. Adaptive terminal sliding mode control scheme for synchronization of fractional-order uncertain chaotic systems. *ISA Trans.* **2020**, *105*, 33–50. [CrossRef]
49. Sun, Z. Synchronization of fractional-order chaotic systems with non-identical orders, unknown parameters and disturbances via sliding mode control. *Chin. J. Phys.* **2018**, *56*, 2553–2559. [CrossRef]
50. Rashidnejad, Z.; Karimaghaee, P. Synchronization of a class of uncertain chaotic systems utilizing a new finite-time fractional adaptive sliding mode control. *Chaos Solitons Fractals X* **2020**, *5*, 100042. [CrossRef]
51. Wang, J.; Shao, C.; Chen, X. Fractional-order DOB-sliding mode control for a class of noncommensurate fractional-order systems with mismatched disturbances. *Math. Methods Appl. Sci.* **2019**, *5*, 1–15. [CrossRef]
52. Wang, J.; Shao, C.; Chen, Y.Q. Fractional order sliding mode control via disturbance observer for a class of fractional order systems with mismatched disturbance. *Mechatronics* **2018**, *53*, 8–19. [CrossRef]
53. Yin, C.; Huang, X.; Chen, Y.; Dadras, S.; Zhong, S.M.; Cheng, Y. Fractional-order exponential switching technique to enhance sliding mode control. *Appl. Math. Modell.* **2017**, *44*, 705–726. [CrossRef]
54. Han, S.I. Fractional-order command filtered backstepping sliding mode control with fractional-order nonlinear disturbance observer for nonlinear systems. *J. Franklin Inst.* **2020**, *357*, 6760–6776. [CrossRef]
55. Ma, T.; Wang, B. Disturbance observer-based Takagi-Sugeno fuzzy control of a delay fractional-order hydraulic turbine governing system with elastic water hammer via frequency distributed model. *Inf. Sci.* **2021**, *569*, 766–785. [CrossRef]
56. Podlubny, I. *Fractional Differential Equations*; Academic Press: New York, NY, USA, 1999.
57. Li, Y.; Chen, Y.Q.; Podlubny, I. Stability of fractional-order nonlinear dynamic systems: Lyapunov direct method and generalized Mittag-Leffler stability. *Comput. Math. Appl.* **2009**, *59*, 1810–1821. [CrossRef]
58. Ran, M.; Wang, Q.; Hou, D. Backstepping design of missile guidance and control based on adaptive fuzzy sliding mode control. *Chin. J. Aeronaut.* **2014**, *27*, 634–642. [CrossRef]